ABSTRACT

Title of thesis: THE CONTROL OF A MATHEMATICAL ANALOG OF A TENTACLE

Xin Xu, Master of Science, 2015

Thesis directed by: Professor William Levine
Department of Electrical and Computer Engineering

A 2-dimensional dynamic analog of squid tentacles was presented. The tentacle analog consists of a multi-cell structure, which can be easily replicated to a large scale. Each cell of the model is a quadrilateral with unit masses at the corners. Each side of the quadrilateral is a spring-damper system in parallel. The spring constants are the controls for the system. The dynamics are subject to the constraint that the area of each quadrilateral must remain constant. The system dynamics was analyzed, and various equilibrium points were found with different controls. Then these equilibrium points were further determined experimentally, demonstrated to be asymptotically stable. A simulation built in MATLAB was used to find the convergence rates under different controls and damping coefficients. Finally, a control scheme was developed and used to drive the system to several configurations observed in real tentacle.

THE CONTROL OF A MATHEMATICAL ANALOG OF A TENTACLE

by

Xin Xu

Thesis submitted to the Faculty of the Graduate School of the
University of Maryland, College Park in partial fulfillment
of the requirements for the degree of
Master of Science
2015

Advisory Committee:
Professor William Levine, Chair/Advisor
Professor Robert Newcomb
Professor Armand Makowski

Acknowledgments

I would like to thank all the people who contributed in some way to the work described in this thesis.

First and foremost, I am greatly indebted to my thesis advisor, Professor William Levine, for giving me an invaluable opportunity to work on this interesting project and for providing me with definite direction, professional guidance and constant encouragement during my research period. It has been a pleasure to work with and learn from such an extraordinary person.

I would like to thank Professor André Tits and Professor P. S. Krishnaprasad for their generous help and suggestions during my entire study period. I am grateful to Professor Jaydev Desai for accepting me to work in his group in my second year so that I have an even better graduate experience. My thanks also go to Professor Robert Newcomb, who supported me and concerned himself with my work. I would also like to thank Professor Armand Makowski for his help on my oral defense.

I would like to thank the staff members, Mrs. Melanie Prange and Mrs. Heather Stewart, for providing advice and support during my study period. The prompt and quality management of Melanie is highly appreciated.

Finally, I must express my profound gratitude to my family and friends who supported me during my time here. I want to thank my parents and my boyfriend for their unfailing support and continuous encouragement throughout these years of study. Thanks go to Miao Zhang, Wenxue Zhao, Yitian Wang, Yue Chen, Zhe Wu and Yang Xie, who made my life in Maryland a lot more fun. Thank you all!

Table of Contents

List of Tables

List of Figures

Chapter 1: Introduction

1.1 Objective of Study

The overall objective of the project is to explore the control of a tentacle using a simpler mathematical analog. The specific objectives are:

- To build a mathematical analog of a tentacle.
- To determine the equilibrium configurations of the tentacle system.
- To determine the stability of the equilibrium points and the rate of convergence.
- To find a family of controls of the tentacle analog.

1.2 Background and Motivation

Elephant's trunks, squid tentacles, and the tongues of many creatures, including humans, have two common features. They are capable of an elaborate and complex collection of movements, and they consist almost entirely of muscles. Muscles can only cause themselves to contract. Some outside force is required to lengthen a muscle. Because muscle is about 85% water and water is incompressible, this

lengthening force is provided by hydrostatic pressure in these boneless structures.

People have studied these muscular hydrostats experimentally and by computer simulations. Simulations can replicate some, but not all, of their movement repertoire, but they provide little insight into their control.

In order to obtain a better understanding of this control issue, this thesis presents a 2-dimensional mathematical analog of the tentacle with a simple mechanical structure. The model is composed of quadrilateral cells. Linear springs with controllable spring constants and rest length equal to zero form the boundaries of the cells. Fixed dampers are in parallel to the springs. These cells are constrained to have constant area, regardless of the forces applied to them. It is easy to replicate such a simple cell on the 2-D plane, thus the properties of a model with many cells can be understood once the simple model is well understood. In this report, the tentacle analog is evaluated as a dynamic system. Its equilibrium points are found, and the corresponding stabilities of the equilibrium points are studied. Additionally, a simulation of the tentacle model is built in MATLAB to verify its dynamic performance with the controls derived from the system analysis.

1.3 The Organization of the Thesis

The thesis is divided into six chapters.

Chapter 1 Introduction: This chapter provides a brief background and motivation of the project.

Chapter 2 Literature Review: This chapter illustrates the relevant literatures

and recent research related to the project.

Chapter 3 Tentacle Analog Analysis: This chapter focuses on the tentacle system modeling, and analysis of the system equilibrium configurations for different model.

Chapter 4 Stability and Rate of Convergence: An experimental method is used to determine stability of the system equilibrium points. And the rate of convergence is also studied by analyzing the experiment data.

Chapter 5 The Control of Tentacle Analog: An example of the control of tentacle analog to achieve several movements is presented.

Chapter 6 Conclusion and Future Work: Conclusion and suggestions on the future work are discussed.

Chapter 2: Literature Review

Most mammals, birds, fish and lizards have bony skeletons to support their bodies and, under the action of muscles, produce movements. However, there are many animals and animal structures that do not have such rigid bones and consist almost entirely of muscles. A notable example is the tongues of many creatures. Instead, they use 'hydrostatic skeletons' [1] so that the muscle contractions on different parts of the biomechanical structure can change their shapes and create various complex movements.

2.1 Muscular Hydrostats

2.1.1 Structure of Muscular Hydrostats

Muscles are composed primarily of water and are essentially incompressible at physiological pressures, thus the structures that consist mainly of muscles without the support of skeletons are termed as muscular hydrostats [2]. A muscular hydrostat is characterized as an array of compactly arranged musculature. Animals and animal structures with such mechanism are often in cylindrical shapes [3]. And the muscles in these cylinders are well-arranged so that the cylinder lengths and diameters can

be actively controlled [1]. There are mainly three orientations for the arrangement of muscles, that are perpendicular to the longitudinal axis (See Fig.2.1):

- Circular: the muscle fibers enclose the cylinder circumferentially.
- Radial: the muscles start at the central axis and extend to the cylinder surface,
- Transverse: the muscle fibers extend in two perpendicular directions along the cross section of the cylinder.

All three arrangements are observed to control the diameter successfully. There are also muscles that are parallel to the longitudinal axis. The length of the cylinder can then be changed and determined corresponding to the diameter since the cylinder volume is constrained to be constant.

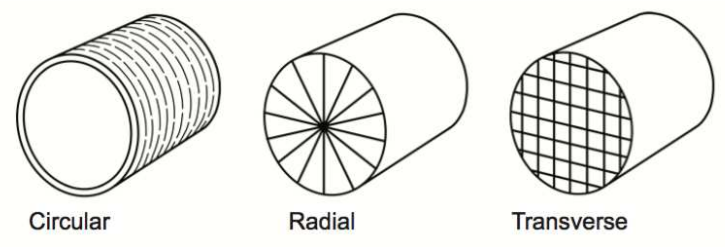

Figure 2.1: Common orientations for muscle fibers in muscular hydrostats [1]

2.1.2 Fundamental Principles

The muscular hydrostat is typically considered as a fluid-filled cavity surrounded by muscle fibers [4]. The most important feature of a muscular hydrostat is that the structure maintains constant volume. Since no evidence is shown that flow of fluid can move in and out of the structure, the muscle tissue is believed to

be incompressible at physiological pressures. In addition, muscle contraction does not change structure volume, which means any change in one dimension will result in passive changes in other dimensions.

2.1.3 Movements in Muscular Hydrostats

The fundamental principle of a muscular hydrostat serves as the basis for achieving a variety of movements. And these movements can be categorized as

- **Lengthening**: The contraction of circular, radial and transverse muscles which are perpendicular to the longitudinal axis will decrease the diameter of the cylinder, and in the meantime increase the pressure inside the structure. Due to the constant volume of the fluid inside the muscle, the dimension on the longitudinal direction must be increased. Then the 'cylinder' is lengthened along the long axis.

- **Shortening**: Contraction of the longitudinal muscles forces the length to decrease but, because of the constant volume constraint, the cross-sectional area (equivalently, the radius of the cylinder increases).

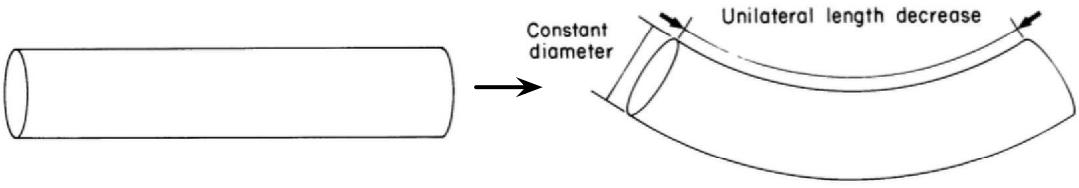

Figure 2.2: Illustration of bending in a muscular hydrostat

- **Bending**: Qualitatively, it can be achieved by muscle contractions only on one side. The unilateral decrease in length together with the constant diameter will resulting in bending towards the muscle contraction side.(See Fig.2.2)

2.2 Some Quantitative Models

The muscular hydrostats mainly consist of muscles, and muscle models have been proposed and thoroughly studied by [5], [6] and many other researchers. However, in order to focus on the functions and properties, a simpler model of muscular hydrostats is needed. After qualitatively understanding the basic structure and properties of the muscular hydrostats, much research was devoted to obtaining quantitative models. Most of the research was from the perspective of biomechanics, thus very complicated biomechanical models were introduced. [7] proposed a model of the reptilian tongue. [8] proposed a dynamic model of squid tentacles. However, the limited number of DOF restricts the model to only describe the lengthening movement. [9] developed a worm-like model. The model is quasi-static, and cannot describe the full dynamics of motion [10].

2.3 Conclusions

The quantitative models proposed are either complicated in the biomechanical structure, or limited in achieving movements. In a word, they are not fully able to characterize the motion of the muscular hydrostat. Thus, it is useful to develop a dynamic model with a simple mathematical form that is able to describe the complex

movements of a muscular hydrostat.

Chapter 3: Tentacle Analog Analysis

3.1 Overview

The tentacle analog is defined on a 2-dimensional plane as an array of cells. Fig.3.1 shows an example. Each cell consists of 4 nodes, and the structure between every two nodes is a spring-damper system in parallel arrangement (Fig.3.2). The mass of each node is concentrated in a point mass and is set as $m = 1$. The springs in the model are defined as massless, linear springs, and the spring constants are defined as the system inputs which can be used to control the tentacle movement and configuration. The damping coefficient of all dampers is b.

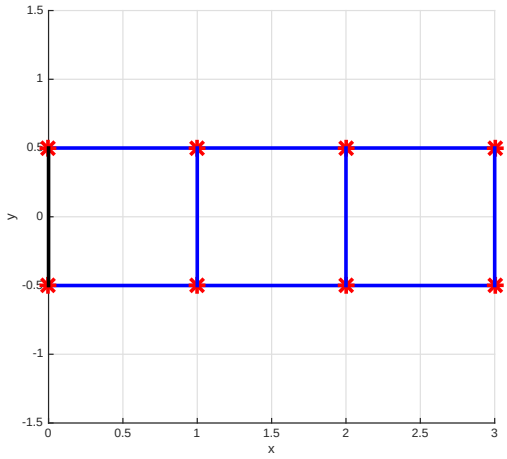

Figure 3.1: A 3-cell, single-row tentacle analog in the initial configuration

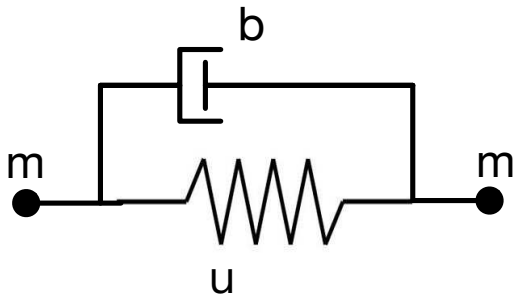

Figure 3.2: The spring-damper system between two nodes

The initial configuration for the tentacle analog is shown in Fig.3.1. And the feasible equilibrium configurations of the tentacle analog in the $x-y$ plane include at least 3 types:

- **Lengthening**: The tentacle is elongating along the x-axis and is thinner in the y-direction.
- **Shortening**: The tentacle is shortened along the x-axis and thickened in the y-axis.
- **Bending**: The tentacle is bending towards one side.

Among these, some special cases are defined. **Pure lengthening** is the case where only the first cell in the model is of a trapezoidal shape while all the other cells are identical rectangles. And **pure shortening** is similar to pure lengthening, but the tentacle contracts to a shorter, thicker shape compared to the inital configuration. There is also **ideal bending**, which is termed as the bended tentacle has a constant radius and forms into a circle. And all the cells have the same area and are identical

isosceles trapezoids in each row.

This chapter focuses on the analysis of the tentacle analog. Two models are thoroughly researched and several theorem are stated and proved.

3.2 Single-row Tentacle Analog

3.2.1 Modeling

A single-row, n-cell tentacle model has $2n+2$ nodes as shown in Fig.3.3 for a 3-cell example. We label the upper (top) $n+1$ nodes as t_i $(i = 1, 2, \ldots, n, n+1)$ and the lower (bottom) $n+1$ nodes as b_i $(i = 1, 2, \ldots, n, n+1)$. Let x_{ti} and x_{bi} $(i = 1, 2, 3, \ldots n, n+1)$ denote the x-position of the $2n+2$ nodes of the tentacle. Similarly, let y_{ti} and y_{bi} be the corresponding y-positions of nodes t_i and b_i. Then, we define

$$\boldsymbol{x} = \begin{bmatrix} \boldsymbol{x_t} \\ \\ \boldsymbol{x_b} \end{bmatrix}$$

and

$$\boldsymbol{y} = \begin{bmatrix} \boldsymbol{y_t} \\ \\ \boldsymbol{y_b} \end{bmatrix}$$

where

$$\boldsymbol{x_\alpha} = \begin{bmatrix} x_{\alpha 1} & x_{\alpha 2} & \ldots & x_{\alpha(n+1)} \end{bmatrix}^T, \ \alpha = t, b$$

$$\boldsymbol{y_\beta} = \begin{bmatrix} y_{\beta 1} & y_{\beta 2} & \ldots & y_{\beta(n+1)} \end{bmatrix}^T, \ \beta = t, b$$

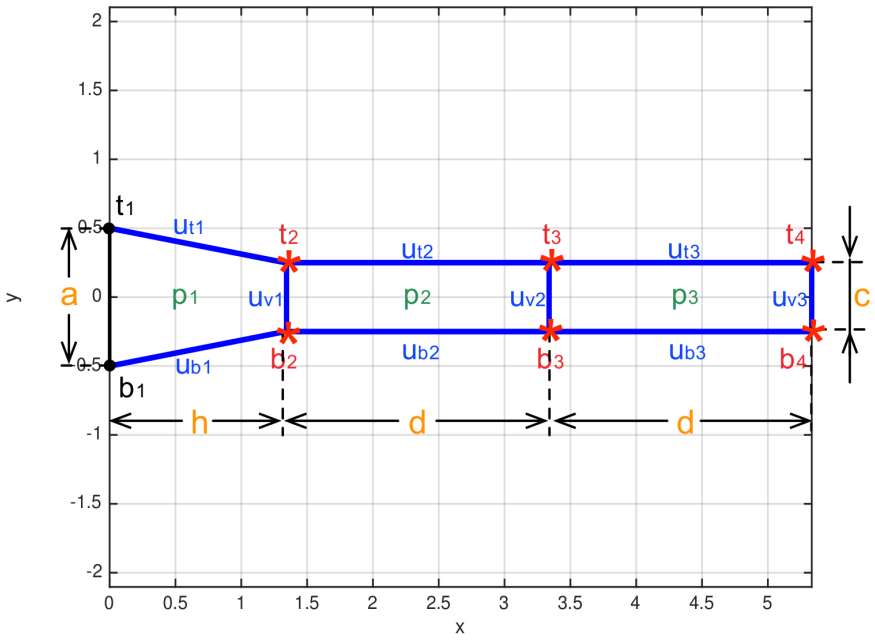

Figure 3.3: Example of a tentacle model with 3 cells shown in the pure lengthening configuration. There are 4 pairs of nodes. The 3 pairs indicated in red and $*$ can move in the $x-y$ plane. The leftmost pair of nodes is fixed and immoveable. There are 9 controls, $u_{\alpha i}$, in blue and 3 pressures, p_i, ($\alpha = t, v, b$ and $i = 1, 2, 3, 4$) shown in green. The lengths for each spring are shown in orange. The controls are the spring constants.

Additionally, the control $\boldsymbol{u}$ and the pressure $\boldsymbol{p}$ are defined by

$$\boldsymbol{u} = \begin{bmatrix} \boldsymbol{u_t} \\ \boldsymbol{u_v} \\ \boldsymbol{u_b} \end{bmatrix}$$

and

$$\boldsymbol{p} = \begin{bmatrix} p_1 & p_2 & \dots & p_n \end{bmatrix}^T$$

where

$$\boldsymbol{u_\gamma} = \begin{bmatrix} u_{\gamma 1} & u_{\gamma 2} & \dots & u_{\gamma n} \end{bmatrix}^T, \ \gamma = t, v, b$$

Here, $\boldsymbol{u_t}, \boldsymbol{u_v}, \boldsymbol{u_b}$ are the controls for the upper, vertical and lower springs. The springs connect the nodes. The controls are the spring coefficients. That is, for example, the force on node t_3 due to control u_{t2} is $u_{t2}\left[(x_{t3} - x_{t2})^2 + (y_{t3} - y_{t2})^2\right]^{1/2}$. And $p_i (i = 1, 2, \dots, n)$ denotes the pressure of the i^{th} cell.

We can first write the dynamics of the n-cell system as

$$\ddot{\boldsymbol{x}} = \mathbf{M}(\boldsymbol{x}, \boldsymbol{y}, \boldsymbol{u}, \boldsymbol{p}) + b\mathbf{M}_{damp}(\dot{\boldsymbol{x}}, \dot{\boldsymbol{y}})\boldsymbol{I} \tag{3.1}$$

$$\ddot{\boldsymbol{y}} = \mathbf{N}(\boldsymbol{x}, \boldsymbol{y}, \boldsymbol{u}, \boldsymbol{p}) + b\mathbf{N}_{damp}(\dot{\boldsymbol{x}}, \dot{\boldsymbol{y}})\boldsymbol{I} \tag{3.2}$$

where $\mathbf{M}$ and $\mathbf{N}$ are functions of the state, pressures and input vectors, b is the damping coefficient assumed to be the same everywhere, and $\boldsymbol{I}$ is a $3n \times 1$ column vector with all elements being 1. Since the controls $\boldsymbol{u}$ and the pressures $\boldsymbol{p}$ enter the equations linearly, eqns (3.1) and (3.2) can be rewritten as,

$$\ddot{\boldsymbol{x}} = \hat{\mathbf{M}}(\boldsymbol{x}, \boldsymbol{y}) \begin{bmatrix} \boldsymbol{u} \\ \boldsymbol{p} \end{bmatrix} + b\mathbf{M}_{damp}(\dot{\boldsymbol{x}}, \dot{\boldsymbol{y}})\boldsymbol{I} \tag{3.3}$$

$$\ddot{\boldsymbol{y}} = \hat{\mathbf{N}}(\boldsymbol{x}, \boldsymbol{y}) \begin{bmatrix} \boldsymbol{u} \\ \boldsymbol{p} \end{bmatrix} + b\mathbf{N}_{damp}(\dot{\boldsymbol{x}}, \dot{\boldsymbol{y}})\boldsymbol{I} \tag{3.4}$$

Combine eqns (3.3) (3.4) into a general form,

$$\begin{aligned} \begin{bmatrix} \ddot{\boldsymbol{x}} \\ \ddot{\boldsymbol{y}} \end{bmatrix} &= \begin{bmatrix} \hat{\mathbf{M}}(\boldsymbol{x}, \boldsymbol{y}) \\ \hat{\mathbf{N}}(\boldsymbol{x}, \boldsymbol{y}) \end{bmatrix} \begin{bmatrix} \boldsymbol{u} \\ \boldsymbol{p} \end{bmatrix} + b \begin{bmatrix} \mathbf{M}_{damp}(\dot{\boldsymbol{x}}, \dot{\boldsymbol{y}}) \\ \mathbf{N}_{damp}(\dot{\boldsymbol{x}}, \dot{\boldsymbol{y}}) \end{bmatrix} \boldsymbol{I} \\ &:= \mathbf{A}(\boldsymbol{x}, \boldsymbol{y}) \begin{bmatrix} \boldsymbol{u} \\ \boldsymbol{p} \end{bmatrix} + b\mathbf{A}_{damp}(\dot{\boldsymbol{x}}, \dot{\boldsymbol{y}})\boldsymbol{I} \end{aligned} \tag{3.5}$$

Let $\boldsymbol{z} = \begin{bmatrix} \boldsymbol{z}_1 & \boldsymbol{z}_2 \end{bmatrix}^T$, where

$$\boldsymbol{z}_1 = \begin{bmatrix} x_{t2} & y_{t2} & x_{b2} & y_{b2} & \dots & x_{t(n+1)} & y_{t(n+1)} & x_{b(n+1)} & y_{b(n+1)} \end{bmatrix}^T$$

and

$$\boldsymbol{z}_2 = \begin{bmatrix} \dot{x}_{t2} & \dot{y}_{t2} & \dot{x}_{b2} & \dot{y}_{b2} & \dots & \dot{x}_{t(n+1)} & \dot{y}_{t(n+1)} & \dot{x}_{b(n+1)} & \dot{y}_{b(n+1)} \end{bmatrix}^T$$

Then, eqn(3.5) can be written as,

$$\dot{\boldsymbol{z}} = \begin{bmatrix} \dot{\boldsymbol{z}}_1 \\ \dot{\boldsymbol{z}}_2 \end{bmatrix} = \begin{bmatrix} \boldsymbol{z}_2 \\ \mathbf{A}(\boldsymbol{z}_1) \begin{bmatrix} \boldsymbol{u} \\ \boldsymbol{p} \end{bmatrix} + b\mathbf{A}_{damp}(\boldsymbol{z}_2)\boldsymbol{I} \end{bmatrix} \tag{3.6}$$

where

$$\begin{bmatrix} \boldsymbol{u} \\ \boldsymbol{p} \end{bmatrix} = \begin{bmatrix} u_{t1} \dots u_{tn} & u_{v1} \dots u_{vn} & u_{b1} \dots u_{bn} & p_1 \dots p_n \end{bmatrix}^T$$

The crucial feature of the system is that the area of each cell must be constant for all time regardless of the forces applied to the system. The pressures play the role

of Lagrange multipliers that produce the forces required to maintain these constant cell areas. Thus, there is really one more equation per cell. That equation can be written in either of two ways. Specifically, one can use Bretschneider's formula. Let S denote the area of a general convex quadrilateral,

$$S = \sqrt{(s-a)(s-b)(s-c)(s-d) - abcd \cdot \cos^2(\frac{\alpha+\gamma}{2})}$$

where parameters a, b, c, d, s, α and γ are shown in Fig.3.4. The other expression for

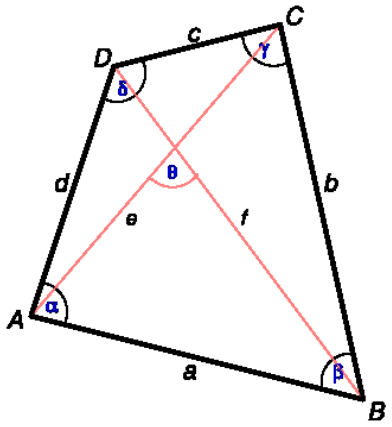

Figure 3.4: A general convex quadrilateral (Wikipedia)

the area of any quadrilateral when the coordinates of its vertices are known is

$$S = \left| \frac{(x_A y_B - y_A x_B) + (x_B y_C - y_B x_C) + (x_C y_D - y_C x_D) + (x_D y_A - y_D x_A)}{2} \right| \quad (3.7)$$

where x_i, y_i are the coordinates for vertex i ($i = A, B, C, D$) of the quadrilateral in Fig.3.4. And the formula actually works for any non-self-intersecting quadrilateral no matter if it is convex or concave. With further analysis, the formula (3.7) was found to not need the absolute value when used for convex quadrilaterals (i.e., it is always negative), and the simplified formula is

$$S = -\frac{(x_A y_B - y_A x_B) + (x_B y_C - y_B x_C) + (x_C y_D - y_C x_D) + (x_D y_A - y_D x_A)}{2} \quad (3.8)$$

Since the coordinates for all nodes in the tentacle model are always known as a fundamental part in the modeling, the second formula for computing the areas is adopted. And S_i is denoted as the area for cell i.

There are additional conditions on both the controls, $\boldsymbol{u}$, and the pressures, $\boldsymbol{p}$. The controls must be nonnegative because they are equivalent to spring coefficients for linear springs. The pressures must be nonnegative as well.

Thus, the complete mathematical description of the tentacle analog is

$$\dot{\boldsymbol{z}} = \begin{bmatrix} \dot{\boldsymbol{z}}_1 \\ \dot{\boldsymbol{z}}_2 \end{bmatrix} = \begin{bmatrix} \boldsymbol{z}_2 \\ \mathbf{A}(\boldsymbol{z}_1) \begin{bmatrix} \boldsymbol{u} \\ \boldsymbol{p} \end{bmatrix} + b\mathbf{A}_{damp}(\boldsymbol{z}_2)\boldsymbol{I} \end{bmatrix}$$

$$S_i = S^* \quad \text{for all } i$$

$$u_{\alpha i} \geq 0 \quad \alpha = t, d \text{ for all time and } i$$

$$p_i \geq 0 \quad \text{for all time and } i$$

where S^* is the constant area.

There are additional constraints that are much more complicated to write and that usually can be ignored. Specifically, all the "spring" lengths must be nonnegative. It is necessary to verify that these constraints are satisfied but they generally are inactive.

3.2.2 Equilibria

Firstly, we analyze the conditions that must be satisfied at a lengthened or shortened equilibrium configuration. If the tentacle can have equilibrium configura-

tions, denoted by $\boldsymbol{z}_{1e}$ with their velocities $\boldsymbol{z}_{2e} = \mathbf{0}$, there must exist some positive controls and pressures such that the states of these configurations are sets of equilibrium points. Then according to eqn(3.6), there should exist $\begin{bmatrix} \boldsymbol{u} \\ \boldsymbol{p} \end{bmatrix}$ that satisfy

$$\mathbf{0} = \begin{bmatrix} \dot{\boldsymbol{z}}_{1e} \\ \dot{\boldsymbol{z}}_{2e} \end{bmatrix} = \begin{bmatrix} \boldsymbol{z}_{2e} \\ \mathbf{A}(\boldsymbol{z}_{1e}) \begin{bmatrix} \boldsymbol{u} \\ \boldsymbol{p} \end{bmatrix} + b\mathbf{A}_{damp}(\boldsymbol{z}_{2e})\boldsymbol{I} \end{bmatrix}$$

which can be reduced to the necessary and sufficient condition

$$\mathbf{A}(\boldsymbol{z}_{1e}) \begin{bmatrix} \boldsymbol{u} \\ \boldsymbol{p} \end{bmatrix} = \mathbf{0} \tag{3.9}$$

for a known $\mathbf{A}(\boldsymbol{z}_{1e})$ because, for linear damping, $\mathbf{A}_{damp}(0) = 0$. Additionally, $\boldsymbol{u}$ and $\boldsymbol{p}$ should satisfy the constraints,

$$\boldsymbol{u} \geq 0 \quad \text{and} \quad \boldsymbol{p} \geq 0 \tag{3.10}$$

and the $\boldsymbol{z}_{1e}$ must form a configuration that complies with

$$S_i = S^* \quad i = 1, 2, \ldots, n \tag{3.11}$$

though the constant value S^* can vary from cell to cell.

To find a nontrivial solution to this problem, the rank of the matrix $\mathbf{A}(\boldsymbol{z}_{1e})$ must be analyzed. If $\mathbf{A}(\boldsymbol{z}_{1e})$ has full rank, which is $4n$, then there is no nontrivial solution to this problem, and the associated configuration can only be an equilibrium point if $\boldsymbol{u}$ and $\boldsymbol{p}$ are both 0. If $\mathbf{A}(\boldsymbol{z}_{1e})$ is less than full rank, there exist infinitely many solutions to eqn(3.9). But it is still necessary to determine if any solution satisfies constraints (3.10) and (3.11).

- **Theorem 1**: For a model consisting of n cells in a single row, in the pure lengthening or pure shortening case, the rank of the $4n \times 4n$ $\mathbf{A}(\boldsymbol{z}_e)$ is $3n$. Furthermore, the u_{ti} $(i = 1, 2, \ldots, n)$ can be chosen to be any numbers greater than or equal to 0 and the remaining controls and the pressures are then uniquely determined.

Proof: Given that the number of cells is n, the dimension of the matrix $\mathbf{A}(\boldsymbol{z}_{1e})$ is $4n \times 4n$. Assume that controls $u_{ti} = \alpha_i$ (for all $1 \leq i \leq n$), where the α_i are arbitrary positive numbers. Then we use induction to solve for the rest of the controls and pressures from cell n to cell 1 for the lengthening and shortening case separately. Due to the configurations of pure lengthening and pure shortening, as can be seen in Fig.3.3 for an example, we know that nodes t_i and b_i $(i = 1, 2, \ldots, n+1\ )$ are symmetric with respect to the x-axis, thus

$$x_{ti} = x_{bi},\ y_{ti} = -y_{bi}$$

Additionally, the parameters for the configuration are

$$x_{t(i+1)} - x_{ti} = \begin{cases} h,\ i = 1 \\ \\ d,\ i \geq 2 \end{cases}$$

$$y_{ti} - y_{bi} = \begin{cases} a,\ i = 1 \\ \\ c,\ i \geq 2 \end{cases}$$

where

$$\frac{a+c}{2}h = cd$$

such that constraint (3.11) is satisfied.

(a) Pure lengthening

- Step 1: For the last cell (cell n), we have four equations governing the positions of nodes $(x_{t(n+1)},\ y_{t(n+1)})$ and $(x_{b(n+1)},\ y_{b(n+1)})$,

$$0 = -\left(x_{t(n+1)} - x_{tn}\right)u_{tn} - \left(x_{t(n+1)} - x_{b(n+1)}\right)u_{vn} + \left|y_{t(n+1)} - y_{b(n+1)}\right| p_n \tag{3.12}$$

$$0 = -\left(y_{t(n+1)} - y_{tn}\right)u_{tn} - \left(y_{t(n+1)} - y_{b(n+1)}\right)u_{vn} + \left|x_{t(n+1)} - x_{tn}\right| p_n \tag{3.13}$$

$$0 = \left(x_{t(n+1)} - x_{b(n+1)}\right)u_{vn} - \left(x_{b(n+1)} - x_{bn}\right)u_{bn} + \left|y_{t(n+1)} - y_{b(n+1)}\right| p_n \tag{3.14}$$

$$0 = \left(y_{t(n+1)} - y_{b(n+1)}\right)u_{vn} - \left(y_{b(n+1)} - y_{bn}\right)u_{bn} + \left|x_{b(n+1)} - x_{bn}\right| p_n \tag{3.15}$$

By rearranging eqns(3.12) and (3.14) (and by symmetry), it is clear that $u_{tn} = u_{bn}$. Then, it is easy to see that eqns(3.13) and (3.15) are equivalent. Thus, we have two linearly independent equations for the last cell with two unknowns, u_{vn} and p_n. Also, the above equations can be rewritten in matrix form,

$$\mathbf{0}_{4\times 1} = \mathbf{A}_n(\boldsymbol{z}_{1en}) \begin{bmatrix} \boldsymbol{u_n} \\ p_n \end{bmatrix} = \begin{bmatrix} -d & 0 & 0 & c \\ 0 & -c & 0 & d \\ 0 & 0 & -d & c \\ 0 & c & 0 & -d \end{bmatrix} \begin{bmatrix} u_{tn} \\ u_{vn} \\ u_{bn} \\ p_n \end{bmatrix}$$

where $\boldsymbol{z}_{1en}$ is the postions of nodes $t_{(n+1)}$ and $b_{(n+1)}$ in the vector form. Then check the rank of $\mathbf{A}_n(\boldsymbol{z}_{1en})$

$$rank(\mathbf{A}_n(\boldsymbol{z}_{1en})) = 3$$

Thus, the above equations have infinitely many solutions. And the null space for $\mathbf{A}_n(\boldsymbol{z}_{1en})$ can be written as

$$N\left(\mathbf{A}_n(\boldsymbol{z}_{1en})\right) = \beta \begin{bmatrix} c/d & d/c & c/d & 1 \end{bmatrix}^T, \quad \beta \in \mathbf{R}$$

If we choose $u_{tn} = \alpha_n$, the system of equations (3.12) (3.13) (3.14) (3.15) has the unique solution,

$$u_{vn} = \left(\frac{d}{c}\right)^2 \alpha_n, \; u_{bn} = \alpha_n, \; p_n = \left(\frac{d}{c}\right) \alpha_n$$

- Step 2: Assume that we have solved for u_t, u_v, u_b and p up to nodes $(x_{t(i+2)},\ y_{t(i+2)})$ and $(x_{b(i+2)},\ y_{b(i+2)})$. Then for nodes $(x_{t(i+1)},\ y_{t(i+1)})$ and $(x_{b(i+1)},\ y_{b(i+1)})$ in cell i, we have four equations,

$$\begin{aligned} 0 =& -(x_{t(i+1)} - x_{ti})u_{ti} + (x_{t(i+2)} - x_{t(i+1)})u_{t(i+1)} \\ & -(x_{t(i+1)} - x_{b(i+1)})u_{vi} + \left|y_{t(i+1)} - y_{b(i+1)}\right| p_i - \left|y_{t(i+1)} - y_{b(i+1)}\right| p_{(i+1)} \end{aligned} \tag{3.16}$$

$$\begin{aligned} 0 =& -(y_{t(i+1)} - y_{ti})u_{ti} + (y_{t(i+2)} - y_{t(i+1)})u_{t(i+1)} - (y_{t(i+i)} - y_{b(i+1)})u_{vi} \\ & + \left|x_{t(i+1)} - x_{ti}\right| p_i + \left|x_{t(i+2)} - x_{t(i+1)}\right| p_{(i+1)} \end{aligned} \tag{3.17}$$

$$\begin{aligned} 0 =& (x_{t(i+1)} - x_{b(i+1)})u_{vi} - (x_{b(i+1)} - x_{bi})u_{bi} + (x_{b(i+2)} - x_{b(i+1)})u_{b(i+1)} \\ & + \left|y_{t(i+1)} - y_{b(i+1)}\right| p_i - \left|y_{t(i+1)} - y_{b(i+1)}\right| p_{(i+1)} \end{aligned} \tag{3.18}$$

$$\begin{aligned} 0 =& (y_{t(i+1)} - y_{b(i+1)})u_{vi} - (y_{b(i+1)} - y_{bi})u_{bi} + (y_{b(i+2)} - y_{b(i+1)})u_{b(i+1)} \\ & - \left|x_{b(i+1)} - x_{bi}\right| p_i - \left|x_{b(i+2)} - x_{b(i+1)}\right| p_{(i+1)} \end{aligned} \tag{3.19}$$

Similarly, by substituting the configuration parameters into the above equa-

tions and rewriting them into the matrix form,

$$\mathbf{0}_{4\times 1} = \mathbf{A}_i(\boldsymbol{z}_{1ei}) \begin{bmatrix} \boldsymbol{u_i} \\ p_i \end{bmatrix} + \mathbf{B}_i(\boldsymbol{z}_{1ei}) \begin{bmatrix} \boldsymbol{u_{(i+1)}} \\ p_{(i+1)} \end{bmatrix}$$

$$= \begin{bmatrix} -d & 0 & 0 & c \\ 0 & -c & 0 & d \\ 0 & 0 & -d & c \\ 0 & c & 0 & -d \end{bmatrix} \begin{bmatrix} u_{ti} \\ u_{vi} \\ u_{bi} \\ p_i \end{bmatrix} + \begin{bmatrix} d & 0 & 0 & -c \\ 0 & 0 & 0 & d \\ 0 & 0 & d & -c \\ 0 & 0 & 0 & -d \end{bmatrix} \begin{bmatrix} u_{t(i+1)} \\ u_{v(i+1)} \\ u_{b(i+1)} \\ p_{n(i+1)} \end{bmatrix}$$

$$= \begin{bmatrix} -d & 0 & 0 & c \\ 0 & -c & 0 & d \\ 0 & 0 & -d & c \\ 0 & c & 0 & -d \end{bmatrix} \begin{bmatrix} u_{ti} \\ u_{vi} \\ u_{bi} \\ p_i \end{bmatrix} + \begin{bmatrix} 0 \\ \alpha_{(i+1)}d^2/c \\ 0 \\ -\alpha_{(i+1)}d^2/c \end{bmatrix}$$

Since $\mathbf{B}_i(\boldsymbol{z}_{1ei}) \begin{bmatrix} \boldsymbol{u_{(i+1)}} \\ p_{(i+1)} \end{bmatrix}$ is in the linear span of matrix $\mathbf{A}_i(\boldsymbol{z}_{1ei})$, the system of equations has infinitely many solutions. Additionally, choosing $u_{ti} = \alpha_i$, results in a unique solution to the above equations,

$$u_{vi} = \left(\frac{d}{c}\right)^2 \left(\alpha_i + \alpha_{(i+1)}\right),\ u_{bi} = \alpha_i,\ p_i = \left(\frac{d}{c}\right)\alpha_i$$

- Step 3: For the first cell of the model, nodes $(x_{t2},\ y_{t2})$ and $(x_{b2},\ y_{b2})$ must satisfy

$$0 = -(x_{t2} - x_{t1})u_{t1} + (x_{t3} - x_{t2})u_{t2} - (x_{t2} - x_{b2})u_{v1} + |y_{t1} - y_{b2}|\, p_1 - |y_{t2} - y_{b2}|\, p_2 \tag{3.20}$$

$$0 = -(y_{t2} - y_{t1})u_{t1} + (y_{t3} - y_{t2})u_{t2} - (y_{t2} - y_{b2})u_{v1} + |x_{t2} - x_{t1}|\, p_1 + |x_{t3} - x_{t2}|\, p_2 \tag{3.21}$$

$$0 = (x_{t2} - x_{b2})u_{v1} - (x_{b2} - x_{b1})u_{b1} + (x_{b3} - x_{b2})u_{b2} + |y_{t1} - y_{b2}|\, p_1 - |y_{t2} - y_{b2}|\, p_2 \tag{3.22}$$

$$0 = (y_{t2} - y_{b2})u_{v1} - (y_{b2} - y_{b1})u_{b1} + (y_{b3} - y_{b2})u_{b2} - |x_{b2} - x_{b1}|\, p_1 - |x_{b3} - x_{b2}|\, p_2 \tag{3.23}$$

which are basically the same as eqns (3.16) (3.17) (3.18) (3.19). And again by substitution with the configuration parameters, we obtain

$$u_{v1} = \left(\frac{d}{c}\right)^2 \alpha_2 + \left[\frac{a-c}{2c} + \frac{2h^2}{c(a+c)}\right]\alpha_1,\ u_{b1} = \alpha_1,\ p_1 = \left(\frac{2h}{a+c}\right)\alpha_1$$

given $u_{t1} = \alpha_1$. Since a is greater than c in the lengthening configuration, it is easy to verify that all controls and pressures are greater than 0, and that the constraint (3.10) is satisfied for all solutions.

To conclude, each pair of nodes of the model has three linearly independent equations governing its position. For a system of n cells, there are n pairs of nodes to be determined. Thus we have $3n$ linearly independent equations. Therefore, for the $4n \times 4n$ matrix $\mathbf{A}(\boldsymbol{z}_{1e})$, its rank is $3n$.

(b) Pure shortening (we analyze this case in the same manner as in the lengthening case)

- Step 1: For cell n, there are four equations governing the positions of the last pair of nodes. They are exactly the same as eqns(3.12) (3.13) (3.14) and (3.15). Thus the same result is obtained. There are only three linearly independent equations. And the unique solution to these equations is

$$u_{vn} = \left(\frac{d}{c}\right)^2 \alpha_n,\ u_{bn} = \alpha_n,\ p_n = \left(\frac{d}{c}\right) \alpha_n$$

given the arbitrarily chosen control $u_{tn} = \alpha_n > 0$.

- Step 2: Assume that all controls u_t, u_v, u_b and pressures p have been solved backwards from cell n to cell $i+1$. We want to solve for the nodes in cell i. We again get eqns(3.16) (3.17) (3.18) and (3.19), which lead to the same conclusion. Only three linearly independent equations will be required. Additionally, given any $u_{ti} = \alpha_i > 0$, by solving the above equations, we obtain

$$u_{vi} = \left(\frac{d}{c}\right)^2 \left(\alpha_i + \alpha_{(i+1)}\right),\ u_{bi} = \alpha_i,\ p_i = \left(\frac{d}{c}\right) \alpha_i$$

- Step 3: For the first cell of the model, eqns (3.20) (3.21) (3.22) (3.23) apply, so three linearly independent equations are again obtained. The solution is

$$u_{v1} = \left(\frac{d}{c}\right)^2 \alpha_2 + \left[\frac{a-c}{2c} + \frac{2h^2}{c(a+c)}\right] \alpha_1,\ u_{b1} = \alpha_1,\ p_1 = \left(\frac{2h}{a+c}\right) \alpha_1$$

Since parameter $a < c$ in the pure shortening case, it is possible that the control u_{v1} is negative. Thus one more condition is needed here to guarantee

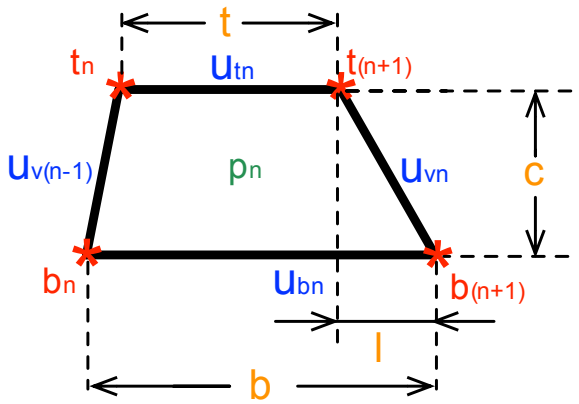

Figure 3.5: A randomly-shaped convex quadrilateral with the top and bottom parallel to each other.

that $u_{v1} > 0$. It is

$$\alpha_2 > \frac{2c^5\left(c^3 - a^2c - 4h^2\right)}{h^2\ (a+c)^3}\alpha_1$$

To conclude, we obtain three linearly independent equations for each pair of nodes in the tentacle model in a pure shortening configuration. For a tentacle model with n cells, there are $3n$ linearly independent equations. Therefore, the rank of the matrix $\mathbf{A}(\boldsymbol{z}_{1e})$ in eqn(3.9) is $3n$.

- **Theorem 2**: For a tentacle model of any size, the last cell can only be a **rectangle** or an **isosceles trapezoid** if the top and bottom of the cell are parallel.

  Proof: Assume that the last cell is a randomly-shaped convex quadrilateral except that the top and bottom are parallel to each other. Without loss of

generality, we can align the x-axis with the top and bottom as shown in Fig.3.5.

Given these assumptions,

$$y_{t(n+1)} - y_{tn} = y_{b(n+1)} - y_{bn} = 0$$

$$y_{t(n+1)} - y_{b(n+1)} = y_{tn} - y_{bn} = c \quad (c > 0)$$

and we can set

$$x_{t(n+1)} - x_{tn} = t \quad (t > 0)$$

$$x_{b(n+1)} - x_{bn} = b \quad (b > 0)$$

$$x_{b(n+1)} - x_{t(n+1)} = l \quad (l \neq 0 \text{ and } l \text{ can be negative})$$

We have four equations defining an equilibrium of the last pair of nodes,

$$0 = -(x_{t(n+1)} - x_{tn})u_{tn} - (x_{t(n+1)} - x_{b(n+1)})u_{vn} + \left|y_{tn} - y_{b(n+1)}\right| p_n$$

$$0 = -(y_{t(n+1)} - y_{tn})u_{tn} - (y_{t(n+1)} - y_{b(n+1)})u_{vn} + \left|x_{b(n+1)} - x_{tn}\right| p_n$$

$$0 = (x_{t(n+1)} - x_{b(n+1)})u_{vn} - (x_{b(n+1)} - x_{bn})u_{bn} + \left|y_{t(n+1)} - y_{bn}\right| p_n$$

$$0 = (y_{t(n+1)} - y_{b(n+1)})u_{vn} - (y_{b(n+1)} - y_{bn})u_{bn} - \left|x_{t(n+1)} - x_{bn}\right| p_n$$

Applying the assumptions to these equations, we get

$$0 = -tu_{tn} + lu_{vn} + cp_n$$

$$0 = -cu_{vn} + (t + l)p_n$$

$$0 = -lu_{vn} - bu_{bn} + cp_n$$

$$0 = \ cu_{vn} - (b - l)p_n$$

which can be rewritten as

$$\mathbf{0}_{4\times 1} = \mathbf{A}_n(\boldsymbol{z}_{en}) \begin{bmatrix} \boldsymbol{u_n} \\ p_n \end{bmatrix} = \begin{bmatrix} -t & l & 0 & c \\ 0 & -c & 0 & l+t \\ 0 & -l & -b & c \\ 0 & c & 0 & l-b \end{bmatrix} \begin{bmatrix} u_{tn} \\ u_{vn} \\ u_{bn} \\ p_n \end{bmatrix} \tag{3.24}$$

To show that there exist some nonzero solutions such that the specific configuration is an equilibrium point, we need to show $\mathbf{A}_n$ is less than full rank. It is easy to see from eqns(3.24) that $rank(\mathbf{A}_n) = 3$ if and only if $b - t = 2l$ holds. And there are 2 cases that satisfy this condition:

- Case 1: The convex quadrilateral is a rectangle if $t = b$ and $l = 0$;
- Case 2: The convex quadrilateral is an isosceles trapezoid if $t \neq b$.

It is obvious that Case 1 is nothing but the configuration for the last cell in the pure lengthening and pure shortening case. And the controls and pressure are

$$u_{vn} = \left(\frac{d}{c}\right)^2 \alpha_1, \;\; u_{bn} = \alpha_1, \;\; p_n = \left(\frac{d}{c}\right) \alpha_1 \tag{3.25}$$

provided $u_{tn} = \alpha_1 \;\; (\alpha_1 > 0)$.

Case 2, where the last cell is an isosceles trapezoid, suggests the possibility of curved equilibria. As a matter of fact, curved equilibria do exist. This is proven below.

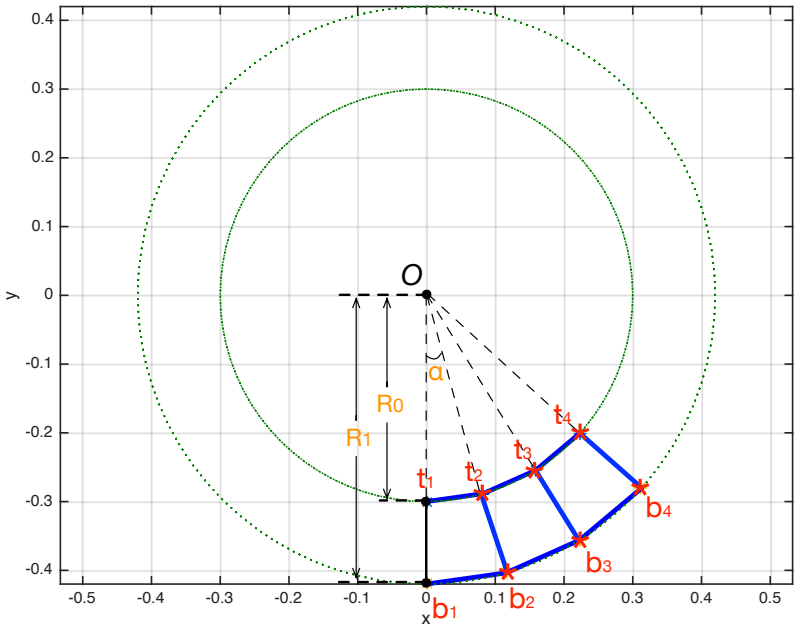

Figure 3.6: Example of a system with 3 cells in the bending case (Each cell is in the shape of an identical isosceles trapezoid. The model has 4 pairs of nodes, where 3 pairs, in red and $*$, can move in the $x-y$ plane. The leftmost pair cannot move. The parameters defining the trapezoidal shape are indicated in orange.)

- **Theorem 3**: Given an n-cell single-row model with an ideal bending configuration $\boldsymbol{z}_{1e}$ consisting of identical isosceles trapezoids , the rank of the $4n \times 4n$ $\mathbf{A}(\boldsymbol{z}_{1e})$ is $3n$. Furthermore, the controls u_{ti} $(i = 1, 2, \ldots, n)$ can be chosen to be any positive number and these choices uniquely determine the other controls and pressures.

  Proof: Mathematical induction is used to prove the bending theorem. Since the designed configuration is bending along a circle with a constant radius , polar coordinates are used for the equilibrium configuration analysis instead of Cartesian coordinates. Similarly, given a system with n cells in the bending configuration $\boldsymbol{z}_{1e}$ with $\boldsymbol{z}_{2e} = \mathbf{0}$, the dimension of the matrix $\mathbf{A}(\boldsymbol{z}_{1e})$ is $4n \times 4n$. Assume that upper controls $u_{ti} = d_i$ (for all $1 \leq i \leq n$), where the d_i are arbitrary positive numbers.

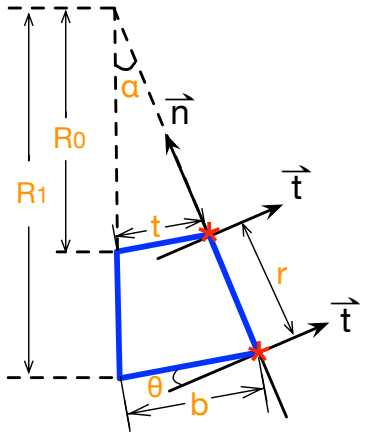

Figure 3.7: Bending configuration of the isosceles trapezoid with the polar coordinates

The isosceles trapezoid is defined by 3 variables, α, R_0 and β as shown in

Fig.3.6 and Fig.3.7. Here, α is the angle between the two legs of the trapezoid ($0 < \alpha < \pi/2$). R_0 is the distance from the upper nodes to the origin O ($R_0 > 0$). And the distance from the bottom nodes to the origin O is denoted as R_1, where R_1 is determined by $R_1 = \beta R_0$ ($\beta > 1$). Without loss of generality, we use variables t, b, θ and r for simplicity (as shown in Fig.3.7), and their relationship with α, R_0 and β is

$$\theta = \frac{\alpha}{2}$$

$$R_1 = \beta R_0$$

$$r = R_1 - R_0 = (\beta - 1)R_0$$

$$t = 2R_0 \sin\theta$$

$$b = 2R_1 \sin\theta = 2\beta R_0 \sin\theta$$

- Step 1: For the last cell (cell n), we have four equations governing the equilibrium of the nodes.

$$0 = -tu_{tn}\cos\theta + rp_n + tp_n \sin\theta$$

$$0 = tu_{tn}\sin\theta - ru_{vn} + tp_n \cos\theta$$

$$0 = -bu_{bn}\cos\theta + rp_n - bp_n \sin\theta$$

$$0 = ru_{vn} + bu_{bn}\sin\theta - bp_n \cos\theta$$

which can be rewritten as

$$\mathbf{0}_{4\times 1} = \mathbf{A}_n(\boldsymbol{z}_{en}) \begin{bmatrix} \boldsymbol{u_n} \\ p_n \end{bmatrix} = \begin{bmatrix} -t\,\cos\theta & 0 & 0 & r + t\,\sin\theta \\ t\,\sin\theta & -r & 0 & t\,\cos\theta \\ 0 & 0 & -b\,\cos\theta & r - b\,\sin\theta \\ 0 & r & b\,\sin\theta & -b\,\cos\theta \end{bmatrix} \begin{bmatrix} u_{tn} \\ u_{vn} \\ u_{bn} \\ p_n \end{bmatrix} \tag{3.26}$$

$$= \begin{bmatrix} -\sin\alpha R_0 & 0 & 0 & (\beta - \cos\alpha)R_0 \\ -(\cos\alpha - 1)R_0 & -(\beta - 1)R_0 & 0 & \sin\alpha R_0 \\ 0 & 0 & -\beta\sin\alpha R_0 & (\beta\cos\alpha - 1)R_0 \\ 0 & (\beta - 1)R_0 & -\beta(\cos\alpha - 1)R_0 & -\beta\sin\alpha R_0 \end{bmatrix} \begin{bmatrix} u_{tn} \\ u_{vn} \\ u_{bn} \\ p_n \end{bmatrix} \tag{3.27}$$

Then, by checking the rank of $\mathbf{A}_n(\boldsymbol{z}_{en})$, we get

$$rank(\mathbf{A}_n(\boldsymbol{z}_{en})) = 3$$

Thus, the above equations have infinitely many solutions. And the null space is

$$N\left(\mathbf{A}_n(\boldsymbol{z}_{en})\right) = \gamma \begin{bmatrix} (\beta - \cos\alpha)\csc\alpha & \frac{(\beta+1)\tan\left(\frac{\alpha}{2}\right)}{\beta - 1} & \cot\alpha - \frac{\csc\alpha}{\beta} & 1 \end{bmatrix}^T, \quad \gamma \in \mathbf{R} \tag{3.28}$$

Additionally, to satisfy constraints (3.10), all the controls and pressures must be nonnegative. Thus, we need all elements in the kernel to be nonnegative.

Then by solving the inequalities

$$(\beta - \cos\alpha)\csc\alpha \geq 0$$
$$\frac{(\beta+1)\tan\left(\frac{\alpha}{2}\right)}{\beta - 1} \geq 0$$
$$\cot\alpha - \frac{\csc\alpha}{\beta} \geq 0$$

Further constraints on variables α and β are obtained. They are

$$0 < \alpha < \pi/2$$

$$\beta > 1/\cos\alpha$$

By the previous assumption that $u_{tn} = d_n$, the controls and pressure for cell n are obtained,

$$u_{vn} = \frac{(\beta+1)\sin\alpha\tan\left(\frac{\alpha}{2}\right)}{(\beta-1)(\beta-\cos\alpha)}d_n$$
$$u_{bn} = \frac{\beta\cos\alpha - 1}{\beta^2 - \beta\cos\alpha}d_n$$
$$p_n = \frac{\sin\alpha}{\beta - \cos\alpha}d_n$$

- Step 2: Assume that we have solved for u_t, u_v, u_b and p from cell n to cell $(i+1)$. Then for nodes $t_{(i+1)}, b_{(i+1)}$ in the i_{th} cell, we have four equations,

$$0 = -tu_{ti}\cos\theta + rp_i + tp_i\sin\theta + tu_{t(i+1)}\cos\theta - rp_{(i+1)} - tp_{(i+1)}\sin\theta$$

$$0 = tu_{ti}\sin\theta - ru_{vi} + tp_i\cos\theta + tu_{t(i+1)}\sin\theta + tp_{(i+1)}\cos\theta$$

$$0 = -bu_{bi}\cos\theta + rp_i - bp_i\sin\theta + bu_{b(i+1)}\cos\theta - rp_{(i+1)} + bp_{(i+1)}\sin\theta$$

$$0 = ru_{vi} + bu_{bi}\sin\theta - bp_i\cos\theta + bu_{b(i+1)}\sin\theta - bp_{(i+1)}\cos\theta$$

By simplification, this system of equations can be rewritten as

$$\mathbf{0}_{4\times 1} = \mathbf{A}_i(\boldsymbol{z}_{ei}) \begin{bmatrix} \boldsymbol{u}_i \\ p_i \end{bmatrix} + \mathbf{B}_i(\boldsymbol{z}_{ei}) \begin{bmatrix} \boldsymbol{u}_{(i+1)} \\ p_{(i+1)} \end{bmatrix} \tag{3.29}$$

$$= \begin{bmatrix} -\sin\alpha R_0 & 0 & 0 & (\beta-\cos\alpha)R_0 \\ -(\cos\alpha-1)R_0 & -(\beta-1)R_0 & 0 & \sin\alpha R_0 \\ 0 & 0 & -\beta\sin\alpha R_0 & (\beta\cos\alpha-1)R_0 \\ 0 & (\beta-1)R_0 & -\beta(\cos\alpha-1)R_0 & -\beta\sin\alpha R_0 \end{bmatrix} \begin{bmatrix} u_{ti} \\ u_{vi} \\ u_{bi} \\ p_i \end{bmatrix} \tag{3.30}$$

$$+ \begin{bmatrix} \sin\alpha R_0 & 0 & 0 & (\cos\alpha-\beta)R_0 \\ -(\cos\alpha-1)R_0 & 0 & 0 & \sin\alpha R_0 \\ 0 & 0 & \beta\sin\alpha R_0 & (1-\beta\cos\alpha)R_0 \\ 0 & 0 & -\beta(\cos\alpha-1)R_0 & -\beta\sin\alpha R_0 \end{bmatrix} \begin{bmatrix} u_{t(i+1)} \\ u_{v(i+1)} \\ u_{b(i+1)} \\ p_{(i+1)} \end{bmatrix}$$

By substitution of controls and pressures solved previously and defining $\boldsymbol{b}_i$ to be

$$\boldsymbol{b}_i = \mathbf{B}_i(\boldsymbol{z}_{ei}) \begin{bmatrix} \boldsymbol{u}_{(i+1)} \\ p_{(i+1)} \end{bmatrix} = \begin{bmatrix} 0 & -\frac{(\beta+1)R_0(\cos\alpha-1)}{\beta-\cos\alpha}d_{(i+1)} & 0 & \frac{(\beta+1)R_0(\cos\alpha-1)}{\beta-\cos\alpha}d_{(i+1)} \end{bmatrix}^T$$

It is easy to see that $\mathbf{A}_i$ computed above is exactly the same as the matrix $\mathbf{A}_n$ in eqn(3.30). Thus its rank is 3 as well. Since the augmented matrix $\begin{bmatrix} \mathbf{A}_i & \boldsymbol{b}_i \end{bmatrix}$ is of the same rank as $\mathbf{A}_i$,

$$rank\left(\begin{bmatrix} \mathbf{A}_i & \boldsymbol{b}_i \end{bmatrix}\right) = rank(\mathbf{A}_i) = 3$$

There exist infinitely many solutions to eqn(3.29). And then by solving for

the equation $\mathbf{A}_i \begin{bmatrix} \boldsymbol{u}_i \\ p_i \end{bmatrix} = -\boldsymbol{b}_i$, the particular solution is given as

$$\begin{bmatrix} u_{ti}^* & u_{vi}^* & u_{bi}^* & p_i^* \end{bmatrix}^T = \begin{bmatrix} 0 & -\frac{(\beta+1)(\cos\alpha-1)}{(\beta-1)(\beta-\cos\alpha)} d_{(i+1)} & 0 & 0 \end{bmatrix}^T$$

Together with the null space acquired from (3.49), and with $u_{ti} = d_i$ $(k_i > 0)$, the controls and pressure can be uniquely determined as

$$\begin{aligned} u_{vi} &= \frac{(\beta+1)\sin\alpha\tan\left(\frac{\alpha}{2}\right)}{(\beta-1)(\beta-\cos\alpha)}(d_i + d_{(i+1)}) \\ u_{bi} &= \frac{\beta\cos\alpha - 1}{\beta^2 - \beta\cos\alpha} d_i \\ p_i &= \frac{\sin\alpha}{\beta-\cos\alpha} d_i \end{aligned}$$

and these are all positive.

- Step 3: For the first cell of the bending model, the equations governing the

positions are the same as eqn(3.29),

$$\mathbf{0}_{4\times1} = \mathbf{A}_1(\boldsymbol{z}_{e1}) \begin{bmatrix} \boldsymbol{u}_1 \\ p_1 \end{bmatrix} + \mathbf{B}_1(\boldsymbol{z}_{e1}) \begin{bmatrix} \boldsymbol{u_2} \\ p_2 \end{bmatrix}$$

$$= \begin{bmatrix} -\sin\alpha R_0 & 0 & 0 & (\beta-\cos\alpha)R_0 \\ -(\cos\alpha-1)R_0 & -(\beta-1)R_0 & 0 & \sin\alpha R_0 \\ 0 & 0 & -\beta\sin\alpha R_0 & (\beta\cos\alpha-1)R_0 \\ 0 & (\beta-1)R_0 & -\beta(\cos\alpha-1)R_0 & -\beta\sin\alpha R_0 \end{bmatrix} \begin{bmatrix} u_{t1} \\ u_{v1} \\ u_{b1} \\ p_1 \end{bmatrix}$$

$$+ \begin{bmatrix} \sin\alpha R_0 & 0 & 0 & (\cos\alpha-\beta)R_0 \\ -(\cos\alpha-1)R_0 & 0 & 0 & \sin\alpha R_0 \\ 0 & 0 & \beta\sin\alpha R_0 & (1-\beta\cos\alpha)R_0 \\ 0 & 0 & -\beta(\cos\alpha-1)R_0 & -\beta\sin\alpha R_0 \end{bmatrix} \begin{bmatrix} u_{t2} \\ u_{v2} \\ u_{b2} \\ p_2 \end{bmatrix}$$

From Step 2, the controls and pressure for the cell 2 are

$$u_{v2} = \frac{(\beta+1)\sin\alpha\tan\left(\frac{\alpha}{2}\right)}{(\beta-1)(\beta-\cos\alpha)}(d_2+d_3)$$
$$u_{b2} = \frac{\beta\cos\alpha-1}{\beta^2-\beta\cos\alpha}d_2$$
$$p_2 = \frac{\sin\alpha}{\beta-\cos\alpha}d_2$$

Then

$$\boldsymbol{b}_1 = \mathbf{B}_1(\boldsymbol{z}_{e1}) \begin{bmatrix} \boldsymbol{u_2} \\ p_2 \end{bmatrix} = \begin{bmatrix} 0 & -\frac{(\beta+1)R_0(\cos\alpha-1)}{\beta-\cos\alpha}d_2 & 0 & \frac{(\beta+1)R_0(\cos\alpha-1)}{\beta-\cos\alpha}d_2 \end{bmatrix}^T$$

Thus, the particular solution of this system of equations is acquired as

$$\begin{bmatrix} u_{ti}^* & u_{vi}^* & u_{bi}^* & p_i^* \end{bmatrix}^T = \begin{bmatrix} 0 & -\frac{(\beta+1)(\cos\alpha-1)}{(\beta-1)(\beta-\cos\alpha)}d_2 & 0 & 0 \end{bmatrix}^T$$

Since the general solution is in the null space of matrix $\mathbf{A}_1(\boldsymbol{z}_{e1})$, it is exactly the result shown in eqn(3.49). The unique solution is

$$u_{v1} = \frac{(\beta+1)\sin\alpha\tan\left(\frac{\alpha}{2}\right)}{(\beta-1)(\beta-\cos\alpha)}(d_1+d_2)$$
$$u_{b1} = \frac{\beta\cos\alpha-1}{\beta^2-\beta\cos\alpha}d_1$$
$$p_1 = \frac{\sin\alpha}{\beta-\cos\alpha}d_1$$

if the control u_{t1} is specified as $u_{t1} = d_1 > 0$.

To conclude, the rank for the coefficient matrix of each cell is 3 in the ideal bending configuration. For a tentacle model with n cells, there are $3n$ linearly independent equations. Therefore, the rank of the matrix $\mathbf{A}(\boldsymbol{z}_e)$ in eqn(3.9) is $3n$. And the controls u_{ti} $(i = 1, 2, \ldots, n)$ can be any positive number.

By Theorem 3, the existence of the bending tentacle configuration is proved. And notice that the model is bending around an origin O with a constant radius.

As a matter of fact, bending into a circle is not the only complex movement that the tentacle model can perform, it can even coil up like real squid tentacles do. This is proven below.

- **Theorem 4**: When the last cell is an isosceles trapezoid at equilibrium, the next to last cell can be a rectangle with all constraints satisfied.

  Proof: Assume the last cell is in the shape of an isosceles trapezoid. And the trapezoid is defined by variables α, β and R_0, as illustrated in Fig.3.8.

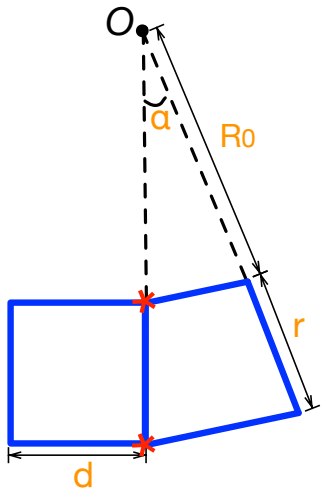

Figure 3.8: A rectangular cell next to an isosceles trapezoidal cell at equilibrium

According to Theorem 3, the controls and pressure for the last cell are

$$
\begin{aligned}
u_{tn} &= d_n \\
u_{vn} &= \frac{(\beta+1)\sin\alpha\tan\left(\frac{\alpha}{2}\right)}{(\beta-1)(\beta-\cos\alpha)}d_n \\
u_{bn} &= \frac{\beta\cos\alpha-1}{\beta^2-\beta\cos\alpha}d_n \\
p_n &= \frac{\sin\alpha}{\beta-\cos\alpha}d_n
\end{aligned}
$$

where d_n can be any positive real number.

The trapezoid cell is connected to a rectangular cell. Due to the constant area constraint, the parameter d for the rectangle satisfies

$$
d = \frac{\frac{1}{2}(\beta^2-1)R_0^2\sin\alpha}{r} = \frac{\frac{1}{2}(\beta^2-1)R_0^2\sin\alpha}{(\beta-1)R_0} = \frac{(\beta+1)R_0}{2}\sin\alpha
$$

Then, for the middle nodes, indicated in red and by $*$, we get

$$\mathbf{0}_{4\times 1} = \mathbf{A}_{(n-1)}(\boldsymbol{z}_{e(n-1)}) \begin{bmatrix} \boldsymbol{u}_{(n-1)} \\ p_{(n-1)} \end{bmatrix} + \mathbf{B}_{(n-1)}(\boldsymbol{z}_{e(n-1)}) \begin{bmatrix} \boldsymbol{u_n} \\ p_n \end{bmatrix}$$

$$= \begin{bmatrix} -\frac{1}{2}(\beta+1)\sin\alpha R_0 & 0 & 0 & (\beta-1)R_0 \\ 0 & -(\beta-1)R_0 & 0 & \frac{1}{2}(\beta+1)\sin\alpha R_0 \\ 0 & 0 & -\frac{1}{2}(\beta+1)\sin\alpha R_0 & (\beta-1)R_0 \\ 0 & (\beta-1)R_0 & 0 & -\frac{1}{2}(\beta+1)\sin\alpha R_0 \end{bmatrix} \begin{bmatrix} u_{t(n-1)} \\ u_{v(n-1)} \\ u_{b(n-1)} \\ p_{(n-1)} \end{bmatrix}$$

$$+ \begin{bmatrix} \sin\alpha R_0 & 0 & 0 & (\cos\alpha-\beta)R_0 \\ -(\cos\alpha-1)R_0 & 0 & 0 & \sin\alpha R_0 \\ 0 & 0 & \beta\sin\alpha R_0 & (1-\beta\cos\alpha)R_0 \\ 0 & 0 & -\beta(\cos\alpha-1)R_0 & -\beta\sin\alpha R_0 \end{bmatrix} \begin{bmatrix} u_{tn} \\ u_{vn} \\ u_{bn} \\ p_n \end{bmatrix}$$

and

$$\boldsymbol{b}_{(n-1)} = \mathbf{B}_{(n-1)}(\boldsymbol{z}_{e(n-1)}) \begin{bmatrix} \boldsymbol{u_n} \\ p_n \end{bmatrix} = \begin{bmatrix} 0 & -\frac{(\beta+1)R_0(\cos\alpha-1)}{\beta-\cos\alpha}d_n & 0 & \frac{(\beta+1)R_0(\cos\alpha-1)}{\beta-\cos\alpha}d_n \end{bmatrix}^T$$

Note that

$$rank\left(\begin{bmatrix} \mathbf{A}_{(n-1)} & \boldsymbol{b}_{(n-1)} \end{bmatrix}\right) = rank(\mathbf{A}_{(n-1)}) = 3$$

which implies infinitely many solutions exist for the above equations. In addition, by solving

$$\mathbf{A}_{(n-1)} \begin{bmatrix} \boldsymbol{u}_{(n-1)} \\ p_{(n-1)} \end{bmatrix} = -\boldsymbol{b}_{(n-1)}$$

the particular solution can be obtained as

$$\begin{bmatrix} u^*_{t(n-1)} & u^*_{v(n-1)} & u^*_{b(n-1)} & p^*_{(n-1)} \end{bmatrix}^T = \begin{bmatrix} 0 & -\frac{(\beta+1)(\cos\alpha-1)}{(\beta-1)(\beta-\cos\alpha)}d_n & 0 & 0 \end{bmatrix}^T$$

And together with the general solution, the controls and pressure for the rectangle cell are

$$
\begin{aligned}
u_{t(n-1)} &= d_{(n-1)} \\
u_{v(n-1)} &= \frac{(\beta+1)^2 \sin^2\alpha}{4(\beta-1)^2} d_{(n-1)} + \frac{(\beta+1)(1-\cos\alpha)}{(\beta-1)(\beta-\cos\alpha)} d_n \\
u_{b(n-1)} &= d_{(n-1)} \\
p_{(n-1)} &= \frac{(\beta+1)\sin\alpha}{2(\beta-1)} d_{(n-1)}
\end{aligned}
$$

Notice that all the solutions are positive if $d_{(n-1)}$ is positive. Thus, there exist feasible controls and pressure that satisfies constraints (3.10) (3.11). In other word, there exist equilibrium configurations in which a rectangular cell is connected with an isosceles trapezoidal cell. Obviously, the rectangular cell can be also connected with other rectangular cells or isosceles trapezoidal cells with different angles α. Thus, the tentacle model could form into a coil.

3.3 Double-row Tentacle Analog

3.3.1 Overview

Now, we analyze the tentacle model with two rows. Here we use similar notation to that for the single-row case. For a double-row tentacle model with n cells per row, there are $3n+3$ nodes in the model. We name the upper (top), middle and lower (bottom) nodes as t_i, m_i and b_i, respectively. Then the positions for these

nodes can be expressed as $\boldsymbol{x}$ and $\boldsymbol{y}$, and

$$\boldsymbol{x} = \begin{bmatrix} \boldsymbol{x_t} \\ \boldsymbol{x_m} \\ \boldsymbol{x_b} \end{bmatrix} \text{ and } \boldsymbol{y} = \begin{bmatrix} \boldsymbol{y_t} \\ \boldsymbol{y_m} \\ \boldsymbol{y_b} \end{bmatrix}$$

where

$$\boldsymbol{x_\alpha} = \begin{bmatrix} x_{\alpha 1} & x_{\alpha 2} & \dots & x_{\alpha(n+1)} \end{bmatrix}^T, \ \alpha = t, m, b$$
$$\boldsymbol{y_\beta} = \begin{bmatrix} y_{\beta 1} & y_{\beta 2} & \dots & y_{\beta(n+1)} \end{bmatrix}^T, \ \beta = t, m, b$$

In addition, the control $\boldsymbol{u}$ and the pressure $\boldsymbol{p}$ are defined as

$$\boldsymbol{u} = \begin{bmatrix} \boldsymbol{u_t} & \boldsymbol{u_{vt}} & \boldsymbol{u_m} & \boldsymbol{u_{vb}} & \boldsymbol{u_b} \end{bmatrix}^T$$

and

$$\boldsymbol{p} = \begin{bmatrix} \boldsymbol{p_t} \\ \boldsymbol{p_b} \end{bmatrix}$$

where

$$\boldsymbol{u_\gamma} = \begin{bmatrix} u_{\gamma 1} & u_{\gamma 2} & \dots & u_{\gamma n} \end{bmatrix}^T, \ \gamma = t, vt, m, vb, b$$
$$\boldsymbol{p_\delta} = \begin{bmatrix} p_{\delta 1} & p_{\delta 2} & \dots & p_{\delta n} \end{bmatrix}^T, \ \delta = t, b$$

Here, $\boldsymbol{u}_t, \boldsymbol{u}_{vt}, \boldsymbol{u}_m, \boldsymbol{u}_{vb}, \boldsymbol{u}_b$ are the controls for springs connecting upper, middle and lower nodes. And p_{ti}, p_{bi} $(i = 1, 2, \dots, n)$ denote the pressure of the i^{th} cell in the upper or lower row, respectively.

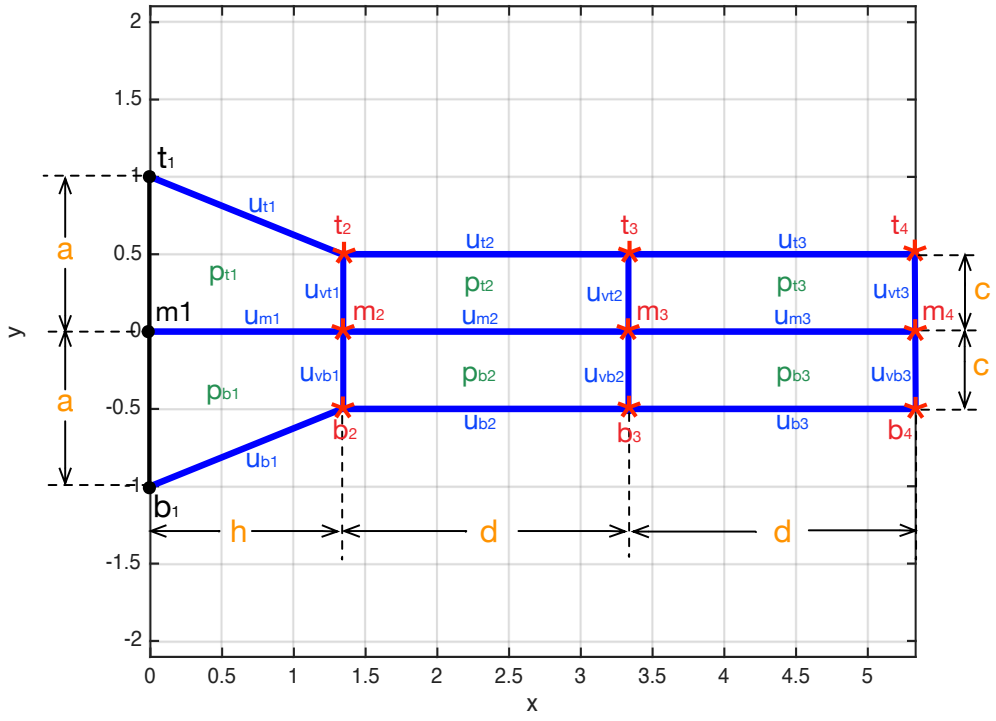

Figure 3.9: Example of a double-row tentacle analog with 3 cells per row in the lengthening case (4 pairs of nodes, where 3 pairs, in red, can move in the $x-y$ plane. 15 controls $u_{\alpha i}$ are indicated in blue while 6 pressures p_i are shown in green ($i = 1, 2, \ldots, n$). The lengths for each spring are shown in orange)

3.3.2 Equilibria

- **Theorem 5**: For the double-row case of the tentacle analog, there exist multiple constant controls and pressures that have the same equilibrium points $\boldsymbol{z}_{1e}$, where

$$\boldsymbol{z}_{1e} = \begin{bmatrix} z_{1e} & z_{2e} & z_{3e} & \dots & z_{ie} & \dots & z_{ne} \end{bmatrix}^T$$

and

$$\boldsymbol{z_{ie}} = \begin{bmatrix} x_{t(i+1)e} & y_{t(i+1)e} & x_{m(i+1)e} & y_{m(i+1)e} & x_{b(i+1)e} & y_{b(i+1)e} \end{bmatrix}^T$$

Analysis: To prove the theorem, we need to show that there exists $[\ \boldsymbol{u}\ \ \boldsymbol{p}\ ]^T$ that satisfy eqn(3.9), eqn(3.10) and eqn(3.11). (The configuration of the double-row tentacle model is illustrated in Fig.3.9, i.e. only the first two cells consisting of the first pairs of nodes is in a trapezoid shape while the rest of the cells are all rectangular, and the tentacle is symmetric about the x-axis. All the parameters of the configuration are shown in Fig.3.9.)

Proof: We prove this theorem in the same manner as we did for the lengthening and shortening case for the single-row tentacle model.

(a) Pure lengthening

- Step 1: For the last pair of nodes $\left(t_{(n+1)},\ m_{(n+1)},\ b_{(n+1)}\right)$, which compose 2

cells, we have 6 equations that governing their positions.

$$0 = -(x_{t(n+1)} - x_{tn})u_{tn} - (x_{t(n+1)} - x_{m(n+1)})u_{vtn} + \left|y_{tn} - y_{m(n+1)}\right| p_{tn} \quad (3.31)$$

$$0 = -(y_{t(n+1)} - y_{tn})u_{tn} - (y_{t(n+1)} - y_{m(n+1)})u_{vtn} + \left|x_{tn} - x_{m(n+1)}\right| p_{tn} \quad (3.32)$$

$$\begin{aligned} 0 = {} & (x_{t(n+1)} - x_{m(n+1)})u_{vtn} - (x_{m(n+1)} - x_{mn})u_{mn} \\ & + (x_{m(n+1)} - x_{b(n+1)})u_{vbn} + \left|y_{t(n+1)} - y_{mn}\right| p_{tn} + \left|y_{mn} - y_{b(n+1)}\right| p_{bn} \end{aligned} \quad (3.33)$$

$$\begin{aligned} 0 = {} & (y_{t(n+1)} - y_{m(n+1)})u_{vtn} - (y_{m(n+1)} - y_{mn})u_{mn} \\ & + (x_{m(n+1)} - x_{b(n+1)})u_{vbn} - \left|x_{t(n+1)} - x_{mn}\right| p_{tn} + \left|x_{mn} - x_{b(n+1)}\right| p_{bn} \end{aligned} \quad (3.34)$$

$$0 = (x_{t(n+1)} - x_{b(n+1)})u_{vbn} - (x_{b(n+1)} - x_{bn})u_{bn} + \left|y_{m(n+1)} - y_{bn}\right| p_n \quad (3.35)$$

$$0 = (y_{t(n+1)} - y_{b(n+1)})u_{vbn} - (y_{b(n+1)} - y_{bn})u_{bn} + \left|x_{m(n+1)} - x_{bn}\right| p_n \quad (3.36)$$

By putting the parameters of this configuration into the equations (3.31) (3.32) (3.33) (3.34) (3.35) (3.36) and simplifying, we obtain

$$\mathbf{0}_{6\times 1} = \mathbf{A}_n(\boldsymbol{z}_{en}) \begin{bmatrix} \boldsymbol{u_n} \\ \boldsymbol{p_n} \end{bmatrix} = \begin{bmatrix} -d & 0 & 0 & 0 & 0 & c & 0 \\ 0 & -c & 0 & 0 & 0 & d & 0 \\ 0 & 0 & -d & 0 & 0 & c & c \\ 0 & c & 0 & -c & 0 & -d & d \\ 0 & 0 & 0 & 0 & -d & 0 & c \\ 0 & 0 & 0 & c & 0 & 0 & -d \end{bmatrix}_{6\times 7} \begin{bmatrix} u_{tn} \\ u_{vtn} \\ u_{mn} \\ u_{vbn} \\ u_{bn} \\ p_{tn} \\ p_{bn} \end{bmatrix}_{7\times 1}$$

Notice that the summation of the second row and the fourth row of the matrix $\mathbf{A}_n(\boldsymbol{z}_{en})$ would cancel the sixth row. We also check the rank of $\mathbf{A}_n(\boldsymbol{z}_{en})$ with the MATLAB symbolic solver and find that $rank\,(\mathbf{A}(\boldsymbol{z}_{en})) = 5$, and

the nullspace is spanned by

$$N\left(\mathbf{A}_n(\boldsymbol{z}_{en})\right) = \begin{bmatrix} \frac{c}{d} & \frac{d}{c} & \frac{c}{d} & 0 & 0 & 1 & 0 \\ 0 & 0 & \frac{c}{d} & \frac{d}{c} & \frac{c}{d} & 0 & 1 \end{bmatrix}^T \begin{bmatrix} \alpha \\ \beta \end{bmatrix}$$

for arbitrary real α, β. Now if we assume $u_{tn} = \alpha_n$ and $u_{bn} = \beta_n$ ($\alpha_n \geq 0, \beta_n \geq 0$), then we can have the controls are

$$u_{vtn} = \left(\frac{d}{c}\right)^2 \alpha_n,\ u_{mn} = \alpha_n + \beta_n,\ u_{vbn} = \left(\frac{d}{c}\right)^2 \beta_n,\ p_{tn} = \frac{d}{c}\alpha_n,\ p_{bn} = \frac{d}{c}\beta_n$$

Since the parameters shown in Fig.3.9 are positive, the controls $\boldsymbol{u_n}$ are non-negative, and satisfy constraint(3.10).

- Step 2: Assume that we have solved for controls $u_t, u_{vt}, u_m, u_{vb}, u_b$ and pressures p_t, p_b from the last pair of nodes backwardly to nodes $t_{(i+2)}$, $m_{(i+2)}$ and

$m_{(i+2)}$. Then for nodes $t_{(i+1)}$, $m_{(i+1)}$ and $b_{(i+1)}$ in cell i, we have six equations,

$$\begin{aligned} 0 = &-(x_{t(i+1)} - x_{ti})u_{ti} + (x_{t(i+2)} - x_{t(i+1)})u_{t(i+1)} \\ &-(x_{t(i+1)} - x_{m(i+1)})u_{vti} + \left|y_{ti} - y_{m(i+1)}\right| p_{ti} - \left|y_{t(i+2)} - y_{m(i+1)}\right| p_{t(i+1)} \end{aligned} \tag{3.37}$$

$$\begin{aligned} 0 = &-(y_{t(i+1)} - y_{ti})u_{ti} + (y_{t(i+2)} - y_{t(i+1)})u_{t(i+1)} \\ &-(y_{t(i+1)} - y_{m(i+1)})u_{vti} + \left|x_{ti} - x_{m(i+1)}\right| p_{ti} + \left|x_{t(i+2)} - x_{m(i+1)}\right| p_{t(i+1)} \end{aligned} \tag{3.38}$$

$$\begin{aligned} 0 = &(x_{t(i+1)} - x_{m(i+1)})u_{vti} - (x_{m(i+1)} - x_{mi})u_{mi} \\ &+ (x_{m(i+2)} - x_{m(i+1)})u_{m(i+1)} - (x_{m(i+1)} - x_{b(i+1)})u_{vbi} + \left|y_{t(i+1)} - y_{mi}\right| p_{ti} \\ &- \left|y_{t(i+1)} - y_{m(i+2)}\right| p_{t(i+1)} + \left|y_{mi} - y_{b(i+1)}\right| p_{bi} - \left|y_{m(i+2)} - y_{b(i+1)}\right| p_{b(i+1)} \end{aligned} \tag{3.39}$$

$$\begin{aligned} 0 = &(y_{t(i+1)} - y_{m(i+1)})u_{vti} - (y_{m(i+1)} - y_{mi})u_{mi} \\ &+ (y_{m(i+2)} - y_{m(i+1)})u_{m(i+1)} - (y_{m(i+1)} - y_{b(i+1)})u_{vbi} - \left|x_{t(i+1)} - x_{mi}\right| p_{ti} \\ &- \left|x_{t(i+1)} - x_{m(i+2)}\right| p_{t(i+1)} + \left|x_{mi} - x_{b(i+1)}\right| p_{bi} + \left|x_{m(i+2)} - x_{b(i+1)}\right| p_{b(i+1)} \end{aligned} \tag{3.40}$$

$$\begin{aligned} 0 = &(x_{m(i+1)} - x_{b(i+1)})u_{vbi} - (x_{b(i+1)} - x_{bi})u_{bi} \\ &+ (x_{b(i+2)} - x_{b(i+1)})u_{b(i+1)} + \left|y_{m(i+1)} - y_{bi}\right| p_{bi} - \left|y_{m(i+2)} - y_{b(i+1)}\right| p_{b(i+1)} \end{aligned} \tag{3.41}$$

$$\begin{aligned} 0 = &(y_{m(i+1)} - y_{b(i+1)})u_{vbi} - (y_{b(i+1)} - y_{bi})u_{bi} + (y_{b(i+2)} - y_{b(i+1)})u_{b(i+1)} \\ &- \left|x_{m(i+1)} - x_{bi}\right| p_{bi} - \left|x_{b(i+2)} - x_{b(i+1)}\right| p_{b(i+1)} \end{aligned} \tag{3.42}$$

By simplifying these equations with the given parameters and the controls

determined previously, we get

$$\mathbf{0}_{6\times 1} = \mathbf{A}_i(\boldsymbol{z}_{ei}) \begin{bmatrix} \boldsymbol{u_i} \\ \\ \boldsymbol{p_i} \end{bmatrix} + \mathbf{b}_i$$

$$= \begin{bmatrix} -d & 0 & 0 & 0 & 0 & c & 0 \\ 0 & -c & 0 & 0 & 0 & d & 0 \\ 0 & 0 & -d & 0 & 0 & c & c \\ 0 & c & 0 & -c & 0 & -d & d \\ 0 & 0 & 0 & 0 & -d & 0 & c \\ 0 & 0 & 0 & c & 0 & 0 & -d \end{bmatrix} \begin{bmatrix} u_{ti} \\ \\ u_{vti} \\ \\ u_{mi} \\ \\ u_{vbi} \\ \\ u_{bi} \\ \\ p_{ti} \\ \\ p_{bi} \end{bmatrix} + \begin{bmatrix} 0 \\ \\ \frac{d^2}{c}\alpha_{(i+1)} \\ \\ 0 \\ \\ \frac{d^2}{c}(\beta_{(i+1)} - \alpha_{(i+1)}) \\ \\ 0 \\ \\ -\frac{d^2}{c}\beta_{(i+1)} \end{bmatrix}$$

It is obvious that $\mathbf{A}_i(\boldsymbol{z}_{ei})$ is exactly the same as $\mathbf{A}_n(\boldsymbol{z}_{en})$, so its rank is 5 as well, and we have 2 free variables for this group of equations. Since

$$rank\left(\begin{bmatrix} \mathbf{A}_i(\boldsymbol{z}_{ei}) & \boldsymbol{b}_i \end{bmatrix}\right) = rank(\mathbf{A}_i(\boldsymbol{z}_{ei})) = 3$$

There are infinitely many solutions to the equation. Assume $u_{ti} = \alpha_i$ and $u_{bi} = \beta_i$ $(\alpha_i \geq 0, \beta_i \geq 0)$, then the controls must be

$$u_{vti} = \left(\frac{d}{c}\right)^2 (\alpha_i + \alpha_{(i+1)}),\ u_{mi} = \alpha_i + \beta_i,\ u_{vbi} = \left(\frac{d}{c}\right)^2 (\beta_i + \beta_{(i+1)}),\ p_{ti} = \frac{d}{c}\alpha_i,\ p_{bi} = \frac{d}{c}\beta_i$$

It is easy to see that all the controls are nonnegative.

- Step 3: For the first 2 cells of the tentacle model, the motions of nodes $t_2,\ m_2$

and b_2 are determined by

$$0 = -(x_{t2} - x_{t1})u_{t1} + (x_{t3} - x_{t2})u_{t2} - (x_{t2} - x_{m2})u_{vt1} + |y_{t1} - y_{m2}|\, p_{t1} - |y_{t2} - y_{m2}|\, p_{t2} \tag{3.43}$$

$$0 = -(y_{t2} - y_{t1})u_{t1} + (y_{t3} - y_{t2})u_{t2} - (y_{t2} - y_{m2})u_{vt1} + |x_{t1} - x_{m2}|\, p_{t1} + |x_{t3} - x_{m2}|\, p_{t2} \tag{3.44}$$

$$\begin{aligned} 0 = {} & (x_{t2} - x_{m2})u_{vt1} - (x_{m2} - x_{m1})u_{m1} + (x_{m3} - x_{m2})u_{m2} - (x_{m2} - x_{b2})u_{vb1} \\ & + |y_{t2} - y_{m1}|\, p_{t1} - |y_{t2} - y_{m3}|\, p_{t2} + |y_{m1} - y_{b2}|\, p_{b1} - |y_{m3} - y_{b2}|\, p_{b2} \end{aligned} \tag{3.45}$$

$$\begin{aligned} 0 = {} & (y_{t2} - y_{m2})u_{vt1} - (y_{m2} - y_{m1})u_{m1} + (y_{m3} - y_{m2})u_{m2} - (y_{m2} - y_{b2})u_{vb1} \\ & - |x_{t2} - x_{m1}|\, p_{t1} - |x_{t2} - x_{m3}|\, p_{t2} + |x_{m1} - x_{b2}|\, p_{b1} + |x_{m3} - x_{b2}|\, p_{b2} \end{aligned} \tag{3.46}$$

$$0 = (x_{m2} - x_{b2})u_{vb1} - (x_{b2} - x_{b1})u_{b1} + (x_{b3} - x_{b2})u_{b2} + |y_{m2} - y_{b1}|\, p_{b1} - |y_{m3} - y_{b2}|\, p_{b2} \tag{3.47}$$

$$0 = (y_{m2} - y_{b2})u_{vb1} - (y_{b2} - y_{b1})u_{b1} + (y_{b3} - y_{b2})u_{b2} - |x_{m2} - x_{b1}|\, p_{b1} - |x_{b3} - x_{b2}|\, p_{b2} \tag{3.48}$$

After simplification,

$$\mathbf{0}_{6\times 1} = \mathbf{A}_1(\boldsymbol{z}_{e1}) \begin{bmatrix} \boldsymbol{u_1} \\ \\ \boldsymbol{p_1} \end{bmatrix} + \mathbf{b}_1$$

$$= \begin{bmatrix} -h & 0 & 0 & 0 & 0 & a & 0 \\ a-c & -c & 0 & 0 & 0 & h & 0 \\ 0 & 0 & -h & 0 & 0 & c & c \\ 0 & c & 0 & -c & 0 & -h & h \\ 0 & 0 & 0 & 0 & -h & 0 & a \\ 0 & 0 & 0 & c & c-a & 0 & -h \end{bmatrix} \begin{bmatrix} u_{t1} \\ u_{vt1} \\ u_{m1} \\ u_{vb1} \\ u_{b1} \\ p_{t1} \\ p_{b1} \end{bmatrix} + \begin{bmatrix} 0 \\ \frac{d^2}{c}\alpha_2 \\ 0 \\ \frac{d^2}{c}(\beta_2 - \alpha_2) \\ 0 \\ -\frac{d^2}{c}\beta_2 \end{bmatrix}$$

Here $rank\,(\mathbf{A}(\boldsymbol{z}_{e1})) = 6$, thus we only have 1 free variable. The nullspace is spanned by

$$N\,(\mathbf{A}_n(\boldsymbol{z}_{e1})) = \alpha \begin{bmatrix} \frac{a}{h} & \frac{a^2-ac+h^2}{ch} & \frac{2c}{h} & \frac{a^2-ac+h^2}{ch} & \frac{a}{h} & 1 & 1 \end{bmatrix}^T$$

for any real α. Let $u_{t1} = \alpha_1$ ($\alpha_1 \geq 0$), we then have

$$u_{vt1} = \frac{a^2-ac+h^2}{ac}\alpha_1 + \left(\frac{d}{c}\right)^2 \alpha_2, \quad u_{m1} = \frac{2c}{h}\alpha_1,$$
$$u_{vb1} = \frac{a^2-ac+h^2}{ac}\alpha_1 + \left(\frac{d}{c}\right)^2 \beta_2, \; u_{b1} = \alpha_1, \; p_{t1} = p_{t1} = \frac{h}{a}\alpha_1$$

When $a \geq c$ in the configuration of Fig.3.9 as required by the pure lengthening case, it is always true that all the controls are nonegative and satisfy constraint(3.10).

To conclude, for a double-row tentacle model with n cells per row in the lengthening configuration (shown in Fig.3.9), the dimension of the matrix $\mathbf{A}(\boldsymbol{z}_e)$ is $6n \times 7n$, and

the rank is $5n+1$. Thus there exist infinitely many solutions for the controls such that satisfy eq(3.9). And by the above steps solving for the controls and pressures, it is easy to see that all the controls and pressures are nonnegative, thus they satisfy the constraints(3.10) and (3.11).

(b) Pure shortening

- Step 1: For cell n, there are six equations governing the positions of the last three nodes. They are exactly the same as eqns(3.31) (3.32) (3.33) (3.34) (3.35)and (3.36). Thus the same result is obtained. And the unique solution to these equations is

$$u_{vtn} = \left(\frac{d}{c}\right)^2 \alpha_n,\ u_{mn} = \alpha_n + \beta_n,\ u_{vbn} = \left(\frac{d}{c}\right)^2 \beta_n,\ p_{tn} = \frac{d}{c}\alpha_n,\ p_{bn} = \frac{d}{c}\beta_n$$

if we assume $u_{tn} = \alpha_n$ and $u_{bn} = \beta_n$ $(\alpha_n \geq 0, \beta_n \geq 0)$.

- Step 2: Assume that all controls and pressures have been solved backwards from cell n to cell $i+1$. We want to solve for the nodes in cell i. We again get eqns(3.37) (3.38) (3.39) (3.40) (3.41) and (3.42), which lead to the same conclusion. Additionally, given any $u_{ti} = \alpha_i > 0$ and $u_{bi} = \beta_i > 0$, by solving the above equations, we obtain

$$u_{vti} = \left(\frac{d}{c}\right)^2 (\alpha_i + \alpha_{(i+1)}),\ u_{mi} = \alpha_i + \beta_i,\ u_{vbi} = \left(\frac{d}{c}\right)^2 (\beta_i + \beta_{(i+1)}),\ p_{ti} = \frac{d}{c}\alpha_i,\ p_{bi} = \frac{d}{c}\beta_i$$

- Step 3: For the first two cells of the model, eqns (3.43) (3.44) (3.45) (3.46) (3.47) (3.48) apply, so six linearly independent equations are obtained. Let

$u_{t1} = \alpha_1$ ($\alpha_1 \geq 0$), we then have the unique solution

$$u_{vt1} = \frac{a^2 - ac + h^2}{ac}\alpha_1 + \left(\frac{d}{c}\right)^2 \alpha_2, \quad u_{m1} = \frac{2c}{h}\alpha_1,$$
$$u_{vb1} = \frac{a^2 - ac + h^2}{ac}\alpha_1 + \left(\frac{d}{c}\right)^2 \beta_2, \; u_{b1} = \alpha_1, \; p_{t1} = p_{t1} = \frac{h}{a}\alpha_1$$

Since parameter $a < c$ in the pure shortening case, it is possible that the control u_{v1} is negative. Thus additional conditions are needed here to guarantee that both u_{vt1} and u_{vb1} are nonnegative. And the conditions are

$$\alpha_2 > \frac{4c^3\left(a^2 - ac + h^2\right)}{h^2 a\left(a + c\right)^2}\alpha_1$$

and

$$\beta_2 > \frac{4c^3\left(a^2 - ac + h^2\right)}{h^2 a\left(a + c\right)^2}\alpha_1$$

To conclude, for a double-row tentacle model with n cells per row in the pure shortening configuration, the dimension of the matrix $\mathbf{A}(\boldsymbol{z}_e)$ is $6n \times 7n$, and the rank is $5n + 1$. Thus there exist multiple constant controls and pressures that have the same equilibrium points. And by the above steps solving for the controls and pressures, it is easy to find that all the controls and pressures are nonnegative, thus they satisfy the constraints(3.10) and (3.11).

- **Theorem 6**: For an n-cell double-row model, there exist multiple constant controls and pressures that have the same equilibrium points and these points form an ideal bending tentacle.

Proof: The theorem is proved by induction. Similar to the single-row model, polar coordinates are used here for convenience when analyzing the equilibrium configuration. A system with n cells in the bending configuration $\boldsymbol{z}_{1e}$ and $\boldsymbol{z}_{2e} = \mathbf{0}$ has a

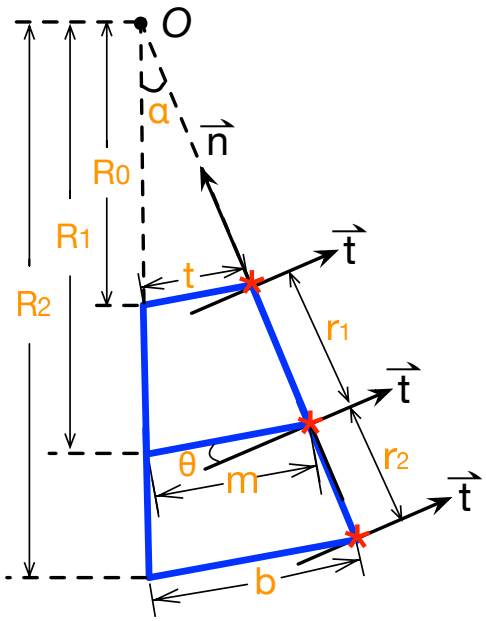

Figure 3.10: Isosceles trapezoid in bending configuration with the polar coordinates

$6n \times 7n$ matrix $\mathbf{A}(\boldsymbol{z}_{1e})$. Assume that the upper controls $u_{ti} = d_i$ (for all $1 \leq i \leq n$), where the d_i are arbitrary positive numbers.

The model in an ideal bending configuration consists of several isosceles trapezoids. The trapezoids in each row are identical. And their shapes are uniquely defined by 3 variables, α, R_0 and β. α is the angle between the two legs of the trapezoid ($0 < \alpha < \pi/2$). R_0 is the distance from the upper nodes to the origin O ($R_0 > 0$). And the distance from the middle nodes to the origin O is denoted as R_1, where R_1 is actually determined by β as $R_1 = \beta R_0$ ($\beta > 1$). R_2 is the distance from the bottom nodes to the origin O. And due to the constant area constraint imposed by the ideal bending, R_2 is fixed once α, R_0 and β are specified. It satisfies

the equation

$$\frac{1}{2}(R_1^2 - R_0^2)\sin\alpha = \frac{1}{2}(R_2^2 - R_1^2)\sin\alpha$$

Thus,

$$R_2 = \sqrt{2R_1^2 - R_0^2} = \sqrt{2\beta^2 - 1}R_0$$

An example of a 3-cell model in the bending configuration can be seen in Fig.3.10. Without loss of generality, alternative variables t, m, b, θ and r_1, r_2 are used for simplicity (shown in Fig.3.10), and their relationship with α, R_0 and β is

$$\begin{aligned}
\theta &= \frac{\alpha}{2} \\
R_1 &= \beta R_0 \\
R_2 &= \sqrt{2\beta^2 - 1}R_0 \\
r_1 &= R_1 - R_0 = (\beta - 1)R_0 \\
r_2 &= R2 - R1 = (\sqrt{2\beta^2 - 1} - \beta + 1)R_0 \\
t &= 2R_0 \sin\theta \\
m &= 2R_1 \sin\theta = 2\beta R_0 \sin\theta \\
b &= 2R_2 \sin\theta = 2(\sqrt{2\beta^2 - 1} - \beta + 1)R_0 \sin\theta
\end{aligned}$$

- Step 1: For the two cells at the unattached end, there are 3 end nodes, i.e., nodes on the boundary of the tentacle model. And the six equations can be acquired by analyzing the states,

$$0 = -tu_{tn}\cos\theta + r_1 p_{tn} + tp_{tn}\sin\theta$$

$$0 = tu_{tn}\sin\theta - r_1 u_{vtn} + tp_{tn}\cos\theta$$

$$0 = -mu_{mn}\cos\theta - mp_{tn}\sin\theta + mp_{bn}\sin\theta + r_1 p_{tn} + r_2 p_{bn}$$

$$0 = mu_{mn}\sin\theta + r_1 u_{vtn} - r_2 u_{vbn} - mp_{tn}\cos\theta + mp_{bn}\cos\theta$$

$$0 = -bu_{bn}\cos\theta + r_2 p_{bn} - bp_{bn}\sin\theta$$

$$0 = r_2 u_{vbn} + bu_{bn}\sin\theta - bp_{bn}\cos\theta$$

which can be rewritten as

$$\mathbf{0}_{6\times 1} = \begin{bmatrix} -t\cos\theta & 0 & 0 & 0 & 0 & r_1 + t\sin\theta & 0 \\ t\sin\theta & -r_1 & 0 & 0 & 0 & t\cos\theta & 0 \\ 0 & 0 & -m\cos\theta & 0 & 0 & r_1 - m\sin\theta & r_2 + m\sin\theta \\ 0 & r_1 & m\sin\theta & -r_2 & 0 & -m\cos\theta & m\cos\theta \\ 0 & 0 & 0 & 0 & -b\cos\theta & 0 & r_2 - b\sin\theta \\ 0 & 0 & 0 & r_2 & b\sin\theta & 0 & -b\cos\theta \end{bmatrix} \begin{bmatrix} u_{tn} \\ u_{vtn} \\ u_{mn} \\ u_{vbn} \\ u_{bn} \\ p_{tn} \\ p_{bn} \end{bmatrix}$$

Then, by checking the rank of the coefficient matrix,

$$rank(\mathbf{A}_n(\boldsymbol{z}_{en})) = 5$$

Thus, the above equations have infinitely many solutions. And the null space

is spanned by

$$N\left(\mathbf{A}_n(\boldsymbol{z}_{en})\right) = \begin{bmatrix} 0 & \beta\csc\alpha - \cot\alpha \\ 0 & \frac{(\beta+1)\tan\left(\frac{\alpha}{2}\right)}{\beta-1} \\ \frac{\sqrt{2\beta^2-1}\csc\alpha}{\beta} - \cot\alpha & \cot\alpha - \frac{\csc\alpha}{\beta} \\ \frac{\left(\beta+\sqrt{2\beta^2-1}\right)\tan\left(\frac{\alpha}{2}\right)}{\sqrt{2\beta^2-1}-\beta} & 0 \\ \cot\alpha - \frac{\beta\csc\alpha}{\sqrt{2\beta^2-1}} & 0 \\ 0 & 1 \\ 1 & 0 \end{bmatrix} \begin{bmatrix} \gamma_1 \\ \gamma_2 \end{bmatrix}, \quad \gamma = \begin{bmatrix} \gamma_1 \\ \gamma_2 \end{bmatrix} \in \mathbf{R}^2 \tag{3.49}$$

Additionally, to satisfy constraints (3.10), all the controls and pressures must be nonnegative. Thus, we need all elements in the kernel to be nonnegative. Then by solving the inequalities, further constraints on variables α and β are obtained as

$$0 < \alpha < \pi/4$$

$$\beta > \cos\alpha\sqrt{\sec(2\alpha)}$$

- Step 2: Assume that we have solved for u_t, u_v, u_b and p from cell n to cell $(i+1)$.

Then for nodes $t_{(i+1)}, m_{(i+1)}, b_{(i+1)}$ in the i_{th} cell, we have six equations,

$$0 = -tu_{ti}\cos\theta + r_1 p_{ti} + tp_{ti}\sin\theta + tu_{t(i+1)}\cos\theta - r_1 p_{t(i+1)} - tp_{t(i+1)}\sin\theta$$

$$0 = tu_{ti}\sin\theta - r_1 u_{vti} + tp_{ti}\cos\theta + tu_{t(i+1)}\sin\theta + tp_{t(i+1)}\cos\theta$$

$$\begin{aligned} 0 = &- mu_{mi}\cos\theta - mp_{ti}\sin\theta + mp_{bi}\sin\theta + r_1 p_{ti} + r_2 p_{bi} + mu_{m(i+1)}\cos\theta \\ &- r_1 p_{t(i+1)} + mp_{t(i+1)}\sin\theta - r_2 p_{b(i+1)} - mp_{b(i+1)}\sin\theta \end{aligned}$$

$$\begin{aligned} 0 = &\, mu_{mi}\sin\theta + r_1 u_{vti} - r_2 u_{vbi} - mp_{ti}\cos\theta + mp_{bi}\cos\theta + mu_{m(i+1)}\sin\theta \\ &- mp_{t(i+1)}\cos\theta + mp_{b(i+1)}\cos\theta \end{aligned}$$

$$0 = -bu_{bi}\cos\theta + r_2 p_{bi} - bp_{bi}\sin\theta + bu_{b(i+1)}\cos\theta - r_2 p_{b(i+1)} + bp_{b(i+1)}\sin\theta$$

$$0 = r_2 u_{vbi} + bu_{bi}\sin\theta - bp_{bi}\cos\theta + bu_{b(i+1)}\sin\theta - bp_{b(i+1)}\cos\theta$$

By simplification, the system of equations above can be rewritten as

$$\mathbf{0}_{6\times 1} = \mathbf{A}_i(\boldsymbol{z}_{ei}) \begin{bmatrix} \boldsymbol{u}_i \\ \boldsymbol{p}_i \end{bmatrix} + \mathbf{B}_i(\boldsymbol{z}_{ei}) \begin{bmatrix} \boldsymbol{u_{(i+1)}} \\ p_{(i+1)} \end{bmatrix}$$

$$= \begin{bmatrix} -t\cos\theta & 0 & 0 & 0 & 0 & r_1 + t\sin\theta & 0 \\ t\sin\theta & -r_1 & 0 & 0 & 0 & t\cos\theta & 0 \\ 0 & 0 & -m\cos\theta & 0 & 0 & r_1 - m\sin\theta & r_2 + m\sin\theta \\ 0 & r_1 & m\sin\theta & -r_2 & 0 & -m\cos\theta & m\cos\theta \\ 0 & 0 & 0 & 0 & -b\cos\theta & 0 & r_2 - b\sin\theta \\ 0 & 0 & 0 & r_2 & b\sin\theta & 0 & -b\cos\theta \end{bmatrix} \begin{bmatrix} u_{ti} \\ u_{vti} \\ u_{mi} \\ u_{vbi} \\ u_{bi} \\ p_{ti} \\ p_{bi} \end{bmatrix}$$

$$+ \begin{bmatrix} t\cos\theta & 0 & 0 & 0 & 0 & -r_1 - t\sin\theta & 0 \\ t\sin\theta & 0 & 0 & 0 & 0 & t\cos\theta & 0 \\ 0 & 0 & m\cos\theta & 0 & 0 & -r_1 + m\sin\theta & -r_2 - m\sin\theta \\ 0 & 0 & m\sin\theta & 0 & 0 & -m\cos\theta & m\cos\theta \\ 0 & 0 & 0 & 0 & b\cos\theta & 0 & -r_2 + b\sin\theta \\ 0 & 0 & 0 & 0 & b\sin\theta & 0 & -b\sin\theta \end{bmatrix} \begin{bmatrix} u_{t(i+1)} \\ u_{vt(i+1)} \\ u_{m(i+1)} \\ u_{vb(i+1)} \\ u_{b(i+1)} \\ p_{t(i+1)} \\ p_{b(i+1)} \end{bmatrix}$$

By computation, one sees that $\mathbf{A}_i$ is exactly the same as the matrix $\mathbf{A}_n$, thus its rank is 5 as well. And because the augmented matrix $\begin{bmatrix} \mathbf{A}_i & \boldsymbol{b}_i \end{bmatrix}$ is of the same rank as $\mathbf{A}_i$,

$$rank\left(\begin{bmatrix} \mathbf{A}_i & \boldsymbol{b}_i \end{bmatrix}\right) = rank(\mathbf{A}_i) = 3$$

Thus, there exist infinitely many solutions to the this equation.

- Step 3: For the first cell of the bending model, the equations governing the positions are same as the equation in Step 2,

$$\mathbf{0}_{6\times 1} = \mathbf{A}_1(\boldsymbol{z}_{e1}) \begin{bmatrix} \boldsymbol{u}_1 \\ \boldsymbol{p}_1 \end{bmatrix} + \mathbf{B}_1(\boldsymbol{z}_{e1}) \begin{bmatrix} \boldsymbol{u_2} \\ p_2 \end{bmatrix}$$

$$= \begin{bmatrix} -t\cos\theta & 0 & 0 & 0 & 0 & r_1 + t\sin\theta & 0 \\ t\sin\theta & -r_1 & 0 & 0 & 0 & t\cos\theta & 0 \\ 0 & 0 & -m\cos\theta & 0 & 0 & r_1 - m\sin\theta & r_2 + m\sin\theta \\ 0 & r_1 & m\sin\theta & -r_2 & 0 & -m\cos\theta & m\cos\theta \\ 0 & 0 & 0 & 0 & -b\cos\theta & 0 & r_2 - b\sin\theta \\ 0 & 0 & 0 & r_2 & b\sin\theta & 0 & -b\cos\theta \end{bmatrix} \begin{bmatrix} u_{t1} \\ u_{vt1} \\ u_{m1} \\ u_{vb1} \\ u_{b1} \\ p_{t1} \\ p_{b1} \end{bmatrix}$$

$$+ \begin{bmatrix} t\cos\theta & 0 & 0 & 0 & 0 & -r_1 - t\sin\theta & 0 \\ t\sin\theta & 0 & 0 & 0 & 0 & t\cos\theta & 0 \\ 0 & 0 & m\cos\theta & 0 & 0 & -r_1 + m\sin\theta & -r_2 - m\sin\theta \\ 0 & 0 & m\sin\theta & 0 & 0 & -m\cos\theta & m\cos\theta \\ 0 & 0 & 0 & 0 & b\cos\theta & 0 & -r_2 + b\sin\theta \\ 0 & 0 & 0 & 0 & b\sin\theta & 0 & -b\sin\theta \end{bmatrix} \begin{bmatrix} u_{t2} \\ u_{vt2} \\ u_{m2} \\ u_{vb2} \\ u_{b2} \\ p_{t2} \\ p_{b2} \end{bmatrix}$$

As in Step 2, there exist infinitely many constant controls and pressures for the first cell that have the same equilibrium points in the ideal bending configurations.

To conclude, the rank for the coefficient matrix of each cell is 5 in the ideal

bending configurations. For a double-row tentacle with n cells in each row, there are $5n$ linearly independent equations. Therefore, the rank of the matrix $\mathbf{A}(\boldsymbol{z}_e)$ is $5n$. And there exist infinitely many constant controls and pressures for the same equilibrium points in the ideal bending configurations.

Chapter 4: Stability and Rate of Convergence

4.1 Introduction

Having shown that there exist equilibrium states of the tentacle analog, the question arises: Are these equilibria stable, asymptotically stable, or unstable? Furthermore, if they are asymptotically stable, how fast do they converges? These questions are studied in this chapter.

In the absence of the constant area constraint, the tentacle analog collapses to a unique equilibrium state in which all lengths are zero because the system consists only of springs with rest lengths equal to zero and ideal linear dampers. Thus, the stability question is really the stability on a very complicated manifold.

The first step is to try to understand the manifold on which the system states are constrained to lie. Given an n-cell single-row tentacle, there are $2n$ nodes, or $4n$ coordinate values, that can move in the $x-y$ plane. And the first pair of nodes is fixed. Due to the constant area requirement, n more constraints are introduced into the tentacle analog and thus in fact only $3n$ coordinate values can be determined freely. More specifically, the configuration of each cell will be determined once 7 coordinate values of its nodes are fixed. The remaining one coordinate value is specified by eqn(3.8). Without loss of generality, coordinates $\boldsymbol{x_t}, \boldsymbol{y_t}, \boldsymbol{x_b}$ are given in

the computer experiment, and coordinates $\boldsymbol{y_b}$ are then obtained as,

$$y_{b(i+1)} = \frac{(x_{ti}y_{t(i+1)} - y_{ti}x_{t(i+1)}) + (x_{b(i+1)}y_{bi} - y_{t(i+1)}x_{b(i+1)}) + (x_{bi}y_{ti} - y_{bi}x_{ti}) + 2S^*}{x_{bi} - xt_{t(i+1)}}$$

$$i = 1, \ldots, n$$

With different values for positions $\boldsymbol{x_t}, \boldsymbol{y_t}, \boldsymbol{x_b}$, a different $\boldsymbol{y_b}$ is obtained. And it must lie on a $3n$-dimensional manifold in a $4n$ dimension space. No special geometry of the manifold is evident. In addition, we were unable to find useful literature on stability of systems restricted to a manifold. Thus, the question of stability was studied by computational experiments of the following form:

- Given an equilibrium configuration, keep the controls constant;
- Randomly perturb its states, subject to the requirement that the perturbation satisfies the constant area constraint;
- Repeat many times randomly and study the results.

4.2 Simulation Algorithm

The simulation algorithm uses two loops for solving for the perturbed system dynamics and finding the trajectories of the system states. Basically, the inner loop solves for the pressure for the next states, and the outer loop is used for finding the trajectories. The algorithm is shown below.

- Step 1: Given values of the state $\boldsymbol{z}^{(i)}$, the controls $\boldsymbol{u}^*$, solve for the next step pressures $\boldsymbol{p}^{(i+1)}$ such that the constant area constraint holds.

The system dynamics are

$$\dot{\boldsymbol{z}} = \begin{bmatrix} \dot{\boldsymbol{z}}_1 \\ \dot{\boldsymbol{z}}_2 \end{bmatrix} = \begin{bmatrix} \boldsymbol{z}_2 \\ \mathbf{A}(\boldsymbol{z}_1) \begin{bmatrix} \boldsymbol{u} \\ \boldsymbol{p} \end{bmatrix} + b\mathbf{A}_{damp}(\boldsymbol{z}_2)\boldsymbol{I} \end{bmatrix}$$

There exists a function $\boldsymbol{z}^{(i+1)} = f(\boldsymbol{p})$ if $\boldsymbol{z}^i$ and controls $\boldsymbol{u}^*$ are fixed and unchanged in f. Meanwhile, eqn(3.8) can also be expressed as a function $g : \mathbf{R}^{4n} \to \mathbf{R}^n$, where $g(\boldsymbol{z})$ is the area error vector a_e in the cells and n is the number of cells. Thus, there is a relationship that maps pressure $\boldsymbol{p}$ to the area error $\boldsymbol{a}_e$,

$$(g \circ f) : \mathbf{R}^n \to \mathbf{R}^n$$

Then by solving the equation

$$0 = (g \circ f)(\boldsymbol{p})$$

We obtain $\boldsymbol{p}^*$, the correct pressure at time $i+1$ ($\boldsymbol{p}^{(i+1)}$), and the corresponding state at time $i+1$ can always satisfies the constraints on the areas.

- Step 2: Solve the dynamics for $\boldsymbol{z}^{(i+1)}$ with $\boldsymbol{p}^*$ and $\boldsymbol{u}^*$ using ode4.
- Step 3: Repeat Step1 and Step 2 until iteration time i meets the final time T.

4.3 Simulation Experiments

To analyze the system stability, a simulation was created in MATLAB for a single-row, 3-cell tentacle model.

Firstly, a configuration was given, and the corresponding controls and pressures that made it an equilibrium were computed. Secondly, an initial state condition was provided. The initial states were randomly perturbed from the equilibrium configuration and yet forced to satisfy the area constraint. The velocities in the initial states were always set to be 0. Then, the simulation algorithm was kept running iteratively until the error between the current states and the equilibrium states was less than a certain threshold.

A random number generator (in the range of $[-1, 1]$) was utilized in the code so that the perturbation on the initial state conditions would vary every time. Then, a variable *boundary* was used to determine the range of perturbation. Thus, the perturbed initial states $\boldsymbol{z}^{(0)} \in B_r$, where $B_r = \{\boldsymbol{z}_1 \in R^n \mid \|\boldsymbol{z}_1\| \leq boundary\}$. And the experiment was run with different values of *boundary* to determine the domain of attraction of a specific system.

4.4 Results of Computational Experiments

The experiments were conducted to test the configuration stability with the MATLAB simulation.

To experimentally determine if the system is stable, it is obviously not enough to test with different initial conditions only a few times. Thus, in this experiment, the simulations were run 100 times with different variable values. And the time of iteration was updated and saved when the algorithm was running. Thus the convergence time for every test could be computed.

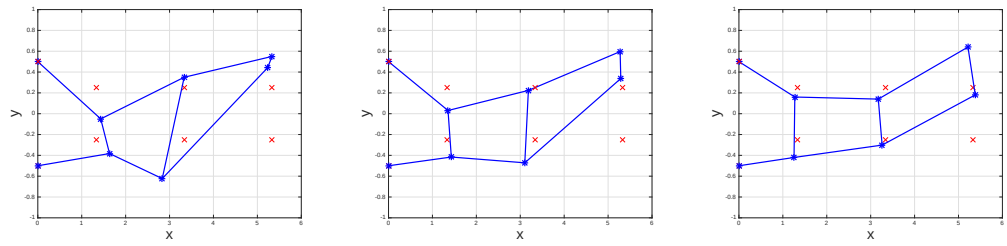

(a) $t = 0s$ (b) $t = 0.5s$ (c) $t = 1.5s$

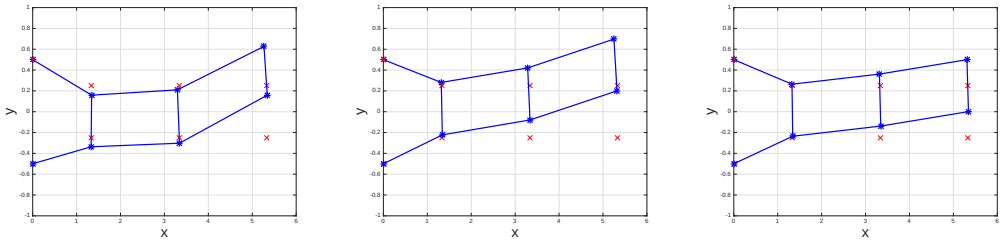

(d) $t = 2.5s$ (e) $t = 11.5s$ (f) $t = 47.0s$

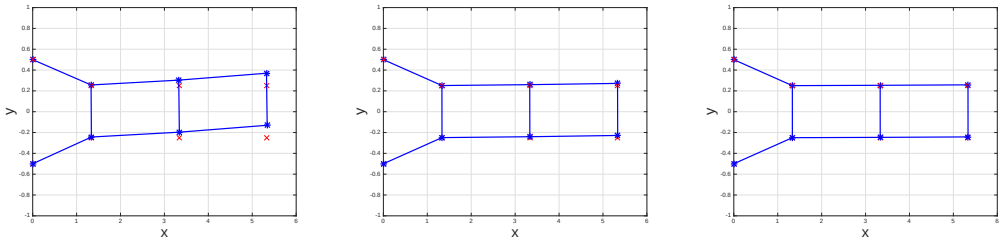

(g) $t = 85.0s$ (h) $t = 172.5s$ (i) $t = 225s$

Figure 4.1: Example of system dynamics with a large initial perturbation.

Since there exist infinitely many constant controls corresponding to each equilibrium configuration, these controls can be scaled with respect to a fundamental vector $\boldsymbol{u}_f$. The controls can then be expressed as

$$\boldsymbol{u} = ratio \cdot \boldsymbol{u}_f$$

where *ratio* is a positive control multiple. The experiments were conducted with various control multiples, *ratio*, and damping coefficients b.

By experiment, we found that the system always converged to the equilibrium configuration from randomly perturbed initial conditions. See Fig.4.1 for an example of the transient response of a 3-cell single-row tentacle analog. The convergence rates for the pure lengthening case can be seen in the following tables.

Tables 4.1 and 4.2 show the simulation results for the convergence time of tentacle models under perturbation using different boundaries on the perturbation. Table 4.1 is the result for a 3-cell single-row tentacle while Table 4.2 is for a 7-cell tentacle. By comparison within each table, it is obvious to see that the convergence time tends to be larger with larger perturbations. Also, by comparison between the two tables, the data shows that with a larger number of cells, it takes much longer for the tentacle to converge to the equilibrium configuration.

Table 4.3 and 4.4 show the convergence time of tentacle models under different control multiple *ratio* and damping coefficients b with certain bounded perturbation. The experiment was conducted with *boundary* being fixed as 0.25, and with *ratio* and b being $1, 4, 7$ and $1, 2, 3$ respectively. Table 4.3 shows the convergence time for tentacles with 3 cells and Table 4.4 is for systems with 7 cells. One sees, from the

boundary		0.25	0.5	1
convergence rate	mean	163.5	188.8	193.5
	max	230.5	253.5	267.5
	min	19.0	25.0	25.0
	std.de.	50.4	48.4	60.0

Table 4.1: Convergence rate (unit: seconds) for 3-cell tentacle with control $ratio = 1$, $b = 1$

boundary		0.25	0.5	1
convergence rate	mean	978.7	1115.0	1320.2
	max	1431.0	1567.5	1694.0
	min	67.0	113.5	139.5
	std.de.	308.6	318.9	251.9

Table 4.2: Convergence rate (unit: seconds) for 7-cell tentacle with control $ratio = 1$, $b = 1$

table, that the convergence is slower when the damping coefficients are increased while keeping the controls unchanged. The result is not surprising because damping generally has the effect of reducing the movement speed of a dynamic system. Notice that with the damping coefficients fixed, the convergence time decreased greatly as the control multiple increased. This phenomenon is explained by the fact that the forces generated by the springs would increase as *ratio* increases, resulting in larger accelerations and faster convergence. Additionally, by observing the transient response of the perturbed system, one finds significant oscillations when large controls (larger *ratio*) are applied. Meanwhile the oscillations was reduced when larger b was introduced into the system.

The equilibrium configuration shown is the pure lengthening case with

$$a = 1$$

$$c = 1/2$$

$$h = 4/3$$

$$d = 2$$

$$S^* = 1$$

control multiple *ratio*		1			4			8		
damping coefficient b		1	2	3	1	2	3	1	2	3
convergence rate	mean	163.5	331.7	510.3	35.5	55.0	117.3	16.7	38.1	61.1
	max	230.0	476.5	729.7	51.5	99.7	175.1	21.8	56.8	86.0
	min	19.0	28.0	60.8	6.9	9.5	6.6	5.0	4.9	8.4
	std.de.	50.4	106.9	149.1	11.8	34.0	39.1	3.9	13.4	16.7

Table 4.3: Convergence rate (unit: second) for perturbed tentacle $n = 3$, perturbation $boundary = 0.25$

control multiple *ratio*		1			4			8		
damping coefficient b		1	2	3	1	2	3	1	2	3
convergence rate	mean	978.7	1937.8	2908.9	218.9	495.2	749.5	98.3	230.6	376.2
	max	1431.0	2898.8	4150.6	314.9	713.4	1129.1	129.3	345.9	531.7
	min	67.0	82.4	1065.0	17.4	51.9	51.4	17.2	24.4	42.0
	std.de.	308.6	747.1	947.9	65.4	136.1	268.9	29.0	93.0	94.8

Table 4.4: Convergence rate (unit: second) for perturbed tentacle $n = 7$, perturbation $boundary = 0.25$

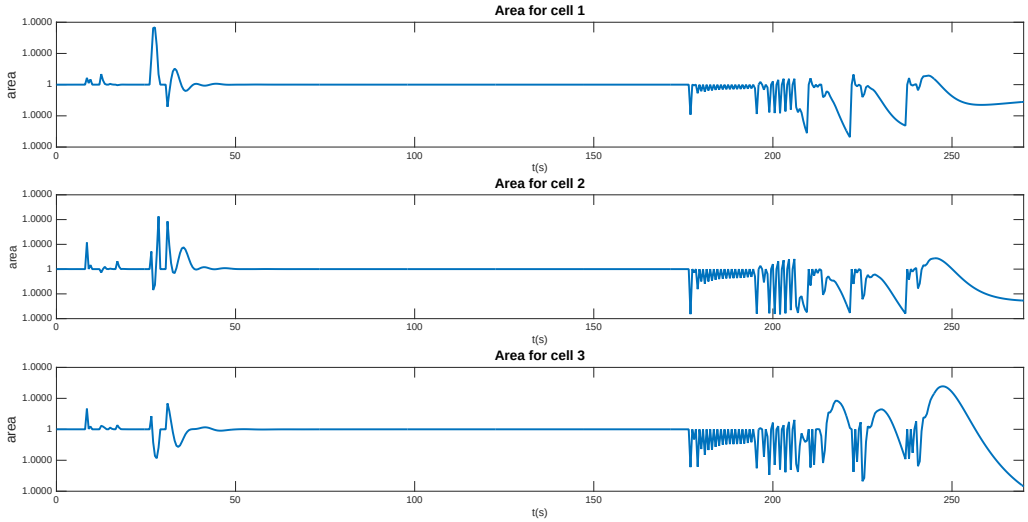

Figure 4.2: Area for cells in a 3-cell tentacle model

During the evolution of the tentacle nodes (system states), it is important to verify that all cells maintain constant area. Thus a function computing the cell areas was run each time as the system evolved. Fig.4.2 is an example for a 3-cell single-row tentacle model that shows the areas remain almost constant at 1 and only change within a range smaller than 0.0001. The test has been conducted with various parameters for several times, and the results are always similar to Fig.4.2. Therefore the constant area constraint holds as the states evolve with time.

4.5 Conclusions

By computational experiment, one can conclude that the tentacle systems studied with specific controls, always converged to the expected equilibrium configuration under considerable perturbations. Thus these equilibrium points are asymptotically stable.

Chapter 5: The Control of Tentacle Analog

In the previous chapters, the controls for the tentacle analog in equilibrium configurations were found. Given different constant controls, the system can maintain specific positions and shapes. In this chapter, an example of controlling a 3-cell, single-row tentacle analog to perform certain movements is presented in Fig.5.1 and Fig.5.2.

Initially, the tentacle analog is static in its original configuration. And the controls are set to shorten the tentacle at $t = 0.1s$. As the tentacle is shortened to the expected configuration at $t = 3s$, the controls are then reset to make the tentacle lengthen. The tentacle reaches its new equilibrium configuration at $t = 9.6s$. Again, we give a new set of controls to the system and make it further lengthen. As seen in Fig.5.1, the tentacle is elongated and becomes even thinner at $t = 20s$. At $t = 20.1s$, the system is controlled to shorten to a previous equilibrium configuration, and it is stabilized at $t = 27s$. After that, at $t = 30s$, the controls are set to make the tentacle bend. And notice that the bending radius is decreasing from $t = 39.6s$ to $t = 64.9s$ as shown in Fig.5.2. The controls input into the system are shown in Fig.5.3.

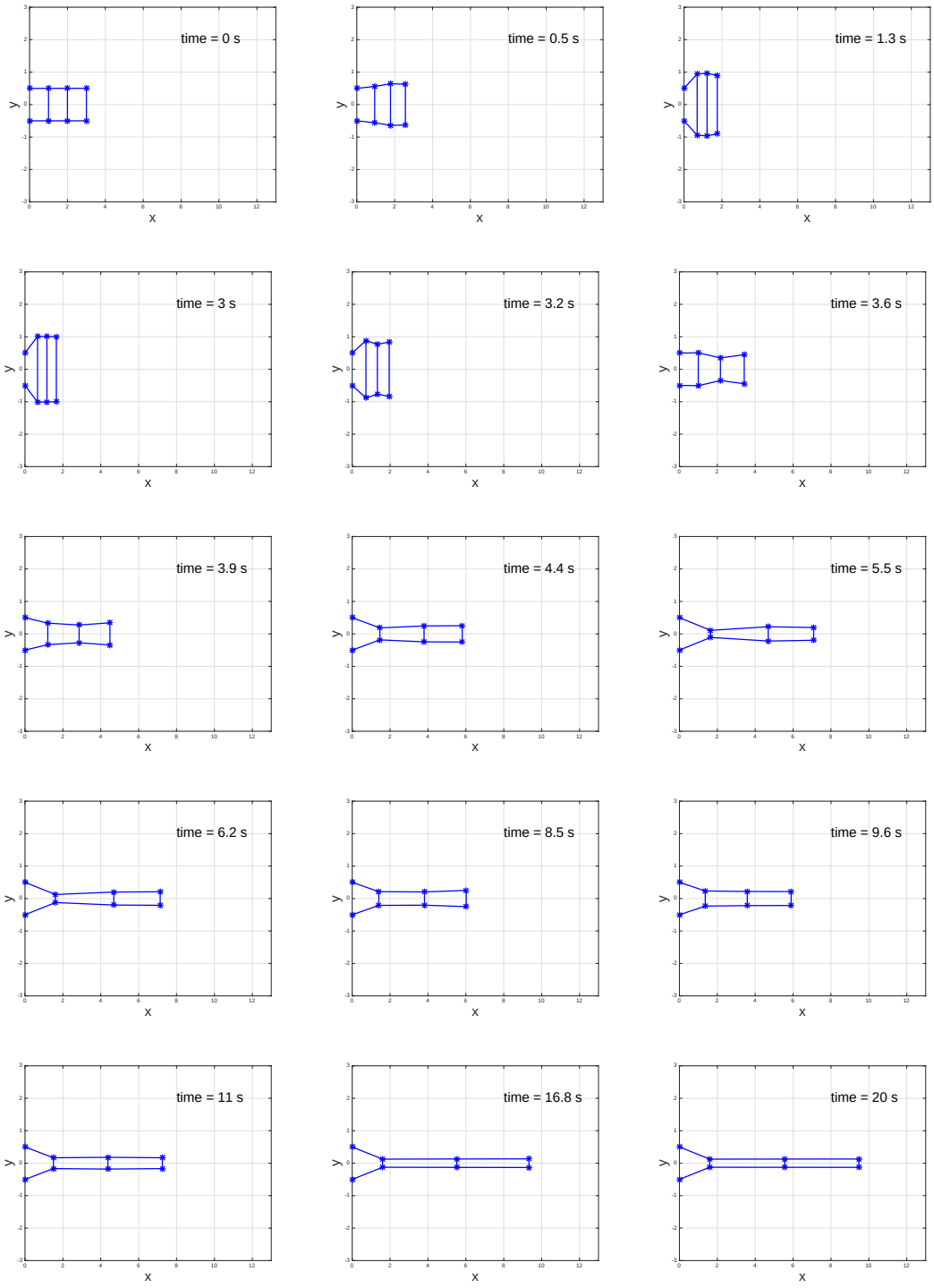

Figure 5.1: The response to the control signals, shown in Fig.5.3, of a 3-cell, single-row tentacle

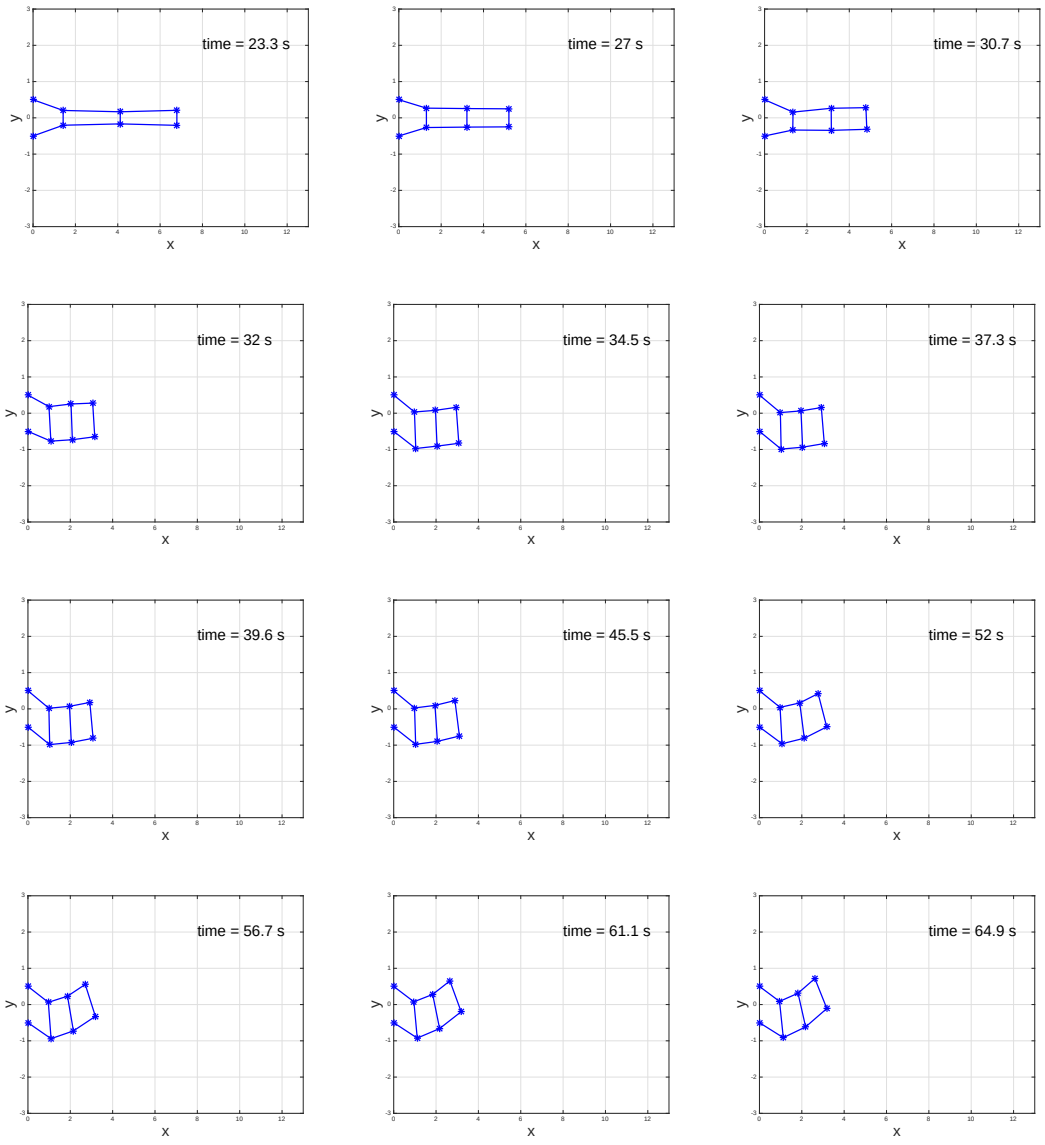

Figure 5.2: The response to the control signals, shown in Fig.5.3, of a 3-cell, single-row tentacle (cont.)

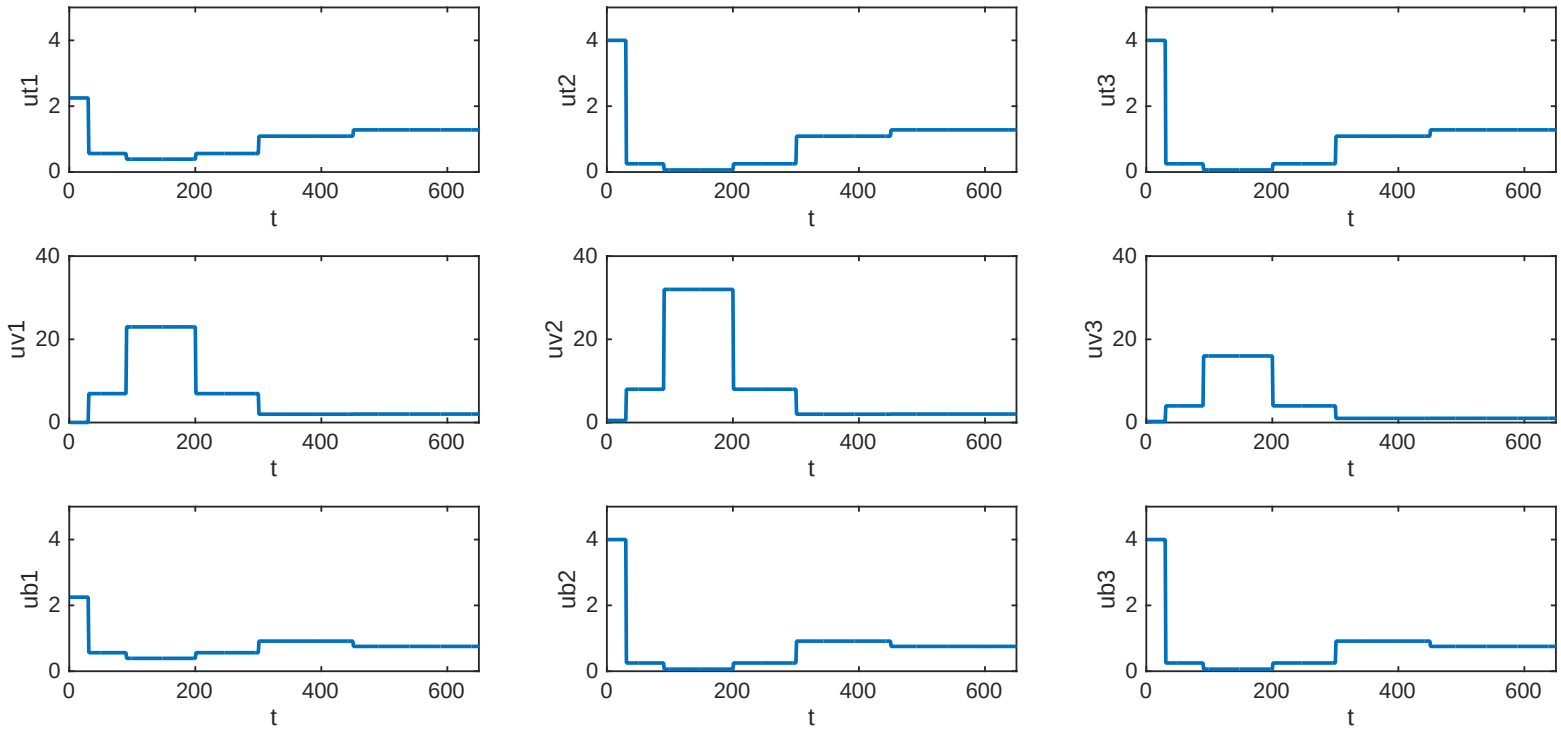

Figure 5.3: The controls for the system

As the entire process of control of the tentacle analog, it is shown that the model can be driven from one equilibrium configuration to another one by changing of controls of the system.

These results suggest that the qualitative understanding of the control of the shape of tentacle and tongues may be incorrect. For the systems analyzed here at equilibrium, one control for each cell can have any positive value provided that all the other controls have exactly the right values. Furthermore, precise movements between equilibria can be produced by controls satisfying the same conditions.

Note that this is similar to the situation for agonist/antagonist pairs of muscles that connect to bones but it is not identical. The presence of bones makes it possible, but not necessary, for one of the pair to be completely inactive. This is apparently not true for muscular hydrostats.

Chapter 6: Conclusions and Future Work

6.1 Conclusions

The work described in this thesis is concerned with the exploration of the control of a tentacle. A 2-dimensional mathematical analog of a tentacle was presented. The model is composed of quadrilateral cells which are constrained to have constant area. The boundaries of the cells are formed by linear springs with controllable spring constants. The model was evaluated as dynamic systems for the single-row case and the double-row case respectively. Equilibrium points and corresponding controls were found for both cases, and they can make the tentacle analog form lengthened, shortened and bent shapes. The stabilities for the equilibrium points were studied with a computational experiment. And they have been demonstrated to be asymptotically stable. A simulation of the tentacle analog was built in MATLAB to verify the dynamic performance with controls derived from the system analysis. The rate of convergence was computed in the simulation, finding that larger controls and smaller damping coefficients resulted in faster convergence. By perturbing the system states and observing the system performance, the domain of attraction for specific equilibrium configurations was also studied. Though the result cannot be provided analytically, it is still safe to say that the domain of attraction is large. In

fact, the experiments are consistent with the domain of attraction being the entire constant area manifold. The simulation was tested with various controls so that the tentacle analog was shown to be able to achieve different movements, including lengthening, shortening and bending.

6.2 Suggestions for Future Work

While this thesis has demonstrated the fundamental functions of the mathematical analog of a tentacle in two dimensional, it could be further developed in a number of ways:

- **Extending the mathematical analog to 3-dimensional space**

  The proposed tentacle analog is a 2-dimensional model that consists of quadrilateral cells with constant area. It can be extended to 3-dimensional space as a model of hexahedral cells with constant volume. All the calculations are feasible in 3-dimensions but are much more complicated. Though more complicated, the extended model is believed to maintain the same functional movements, like lengthening, shortening and bending. And more complicated movements, such as torsion, may to be feasible. Furthermore, the 3-dimensional case can be used as an analog of a tongue. Tongues are much more interesting and important than tentacles.

- **Studying the system performance under the case of environment interaction**

  External forces has not been taken into consideration in the current work.

Thus the tentacle analog used in this thesis does not interact with the environment. This topic should be further analyzed so that the tentacle model could be controlled to manipulate objects in the environment.

- **Analyzing the workspace of the tentacle analog**

  It has been proven that the tentacle analog can be controlled to form different configurations and achieve various complex movements. And the workspace of the tentacle analog remains to be studied.

- **Planning the tentacle movement trajectory**

  Since the tentacle is capable of creating several complex movements, it is of interest to consider optimal control and trajectories of the tentacle analog.

- **Exploring the asymptotics** It would be interesting to study the effects of repeatedly dividing each cell into 4 identical subcells. Making the individual cells smaller while keeping the overall area constant would bring the analog closer to a two dimensional model of a real tentacle.

- **Building a mechanical version** A physical system with the same properties as the tentacle analog might be useful in some applications, especially those requiring complex maneuvers in tight spaces.

Bibliography

[1] William M Kier. The diversity of hydrostatic skeletons. *The Journal of experimental biology*, 215(8):1247–1257, 2012.

[2] Kathleen K Smith and William M Kier. Tongue tentacles and trunks: the biomechanics of movement in muscular hydrostats. *Zool J Linnean Soc*, 83(4):307–324, 1985.

[3] Stephen A Wainwright et al. *Axis and circumference*. Harvard University Press, 1988.

[4] William M Kier. Hydrostatic skeletons and muscular hydrostats. *nautilus*, 8:11, 1992.

[5] AV Hill. The heat of shortening and the dynamic constants of muscle. *Proceedings of the Royal Society of London B: Biological Sciences*, 126(843):136–195, 1938.

[6] Felix E Zajac. Muscle and tendon: properties, models, scaling, and application to biomechanics and motor control. *Critical reviews in biomedical engineering*, 17(4):359–411, 1988.

[7] Hillel J Chiel, Patrick Crago, Joseph M Mansour, and Kamal Hathi. Biomechanics of a muscular hydrostat: a model of lapping by a reptilian tongue. *Biological cybernetics*, 67(5):403–415, 1992.

[8] JL Van Leeuwen and William M Kier. Functional design of tentacles in squid: linking sarcomere ultrastructure to gross morphological dynamics. *Philosophical Transactions of the Royal Society of London B: Biological Sciences*, 352(1353):551–571, 1997.

[9] Martin Wadepuhl and Wolf-Jürgen Beyn. Computer simulation of the hydrostatic skeleton. the physical equivalent, mathematics and application to wormlike forms. *Journal of theoretical biology*, 136(4):379–402, 1989.

[10] Yoram Yekutieli, Roni Sagiv-Zohar, Ranit Aharonov, Yaakov Engel, Binyamin Hochner, and Tamar Flash. Dynamic model of the octopus arm. i. biomechanics of the octopus reaching movement. *Journal of neurophysiology*, 94(2):1443–1458, 2005.